UNIVERSITY OF GENOA
Department of Experimental Medicine
General Pathology Section

Ph.D. in Experimental Medicine

Curriculum *Cellular and molecular pathology of age-related diseases*

XXXII Cycle

"Investigating PLX4032 resistance in a human melanoma cell line: a question of metabolism"

Ph.D. Candidate:

Dott.ssa Ombretta Garbarino

Tutor:

Prof.ssa Cinzia M. Domenicotti

Ph.D. School Coordinator

Prof. Giambattista Bonanno

Academic Year 2018-2019

ABSTRACT

To date, the standard approach to metastatic melanoma with classic chemotherapeutic agents has been unsuccessful. In the last 15 years, he identification of mutations in BRAF genes, such as BRAF^{V600E}, led to the development of BRAF mutant target therapies with small biological inhibitors (i.e. Vemurafenib, PLX4032) that specifically block the constitutively active MAPK-mediated pathway. Although patients respond positively at first, after six-months therapy most patients relapse due to acquired resistance to inhibitors.

The heterogeneity of this tumor makes the study of melanoma acquired resistance more complex, pointing out the importance of directing research towards personalized medicine. Moreover, cancer cells undergo a multifaceted rewiring of cellular metabolism to support their biosynthetic needs, and the implications and clinical relevance in melanoma acquired resistance to PLX4032 has not been elucidated.

For these purposes, in this thesis a human mutant BRAF^{V600E} PLX4032 resistant subline was selected. It is important to note that this selection derives directly from tumor biopsies prior to therapy, and the treatment has been protracted for six months, in order to obtain a truthful model of resistance.

In the first part of the work the acquisition of resistance, together with tumorigenicity, clonogenicity and invasiveness were assessed.

It was also found that P-ERK and MITF, two known mediators of resistance in melanoma, are not overexpressed in the resistant melanoma cell line demonstrating to not mediate PLX4032 resistance.

The second part of the work was focused on the identification of metabolic changes, that could be involved in the acquisition of resistance to BRAF inhibitors.

This thesis highlights some potential key metabolic and phenotypic markers mediating resistance to targeted therapies in cutaneous malignant melanoma, emphasizing the importance to study metabolic changes that could be used as adjuvant target to overcome or bypass acquired resistance.

TABLE OF CONTENTS

_____

_____

LIST OF FIGURES

1 INTRODUCTION

1.1 MELANOMA

Melanoma is a malignancy that arises from the uncontrolled proliferation of melanocytes which are specialized pigment-producing cells of neuroectodermal origin found in the epidermis, meninges, inner ear, leptomeninges and eye [1].

1.1.1 Normal organization of melanocytes

Anatomically, melanocytes are located in the skin, between the epidermidis and the dermis layer, where their function is strictly controlled by keratinocytes (Figure 1). During skin exposure to UV, melanocytes are able to produce melanin, a brown pigment that protects the deeper layer of the skin from harmful UVR-
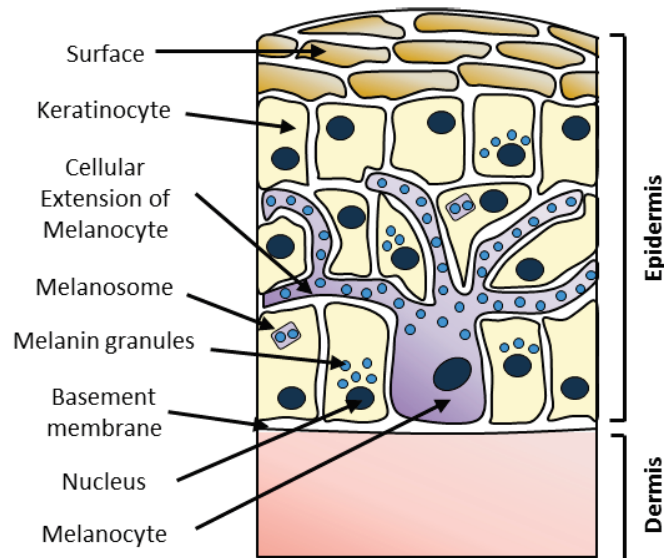
Figure 1. Schematic illustration of normal organization in the epidermis. The structure includes keratinocytes and melanin-producing melanocytes. The melanosomes are transported to neighbour keratinocytes by the extension of melanocytes. The transferred melanin forms a shield against UVR.

generated free radicals, causing the appearance of tanning [2], [3].

In the epidermis under physiological conditions, melanocytes and keratinocytes form the "melanin unit", aligned along the basement

_____

membrane zone. Melanocyte dentrites extends into the upper layers of the epidermis, transporting pigment-containing melanosomes to keratinocytes. Undifferentiated keratinocytes of the basal layer are able to regulate melanocyte growth, number of dendrites and expression of cell surface molecules [4], [5]. This highly-ordered organizational pattern is the structural basis for intercellular regulation, and its organization is only disturbed during transformation into a nevus or a melanoma.

1.1.2 Melanoma development

Melanoma development is considered a multi-step process, and two models of melanoma progression based on clinical and histopathological features has been proposed.

The ***Clark level*** stages are based on the description of the depth of melanoma during its growth in the skin (Figure 2). The first two stages represent the transition from a benign and confined nevus to an uncontrolled growth of normal melanocytes (Dysplastic nevus) with gain of structural atypia. During the radial-growth phase, melanoma has invaded intraepidermally, without showing metastatic property. The loss of expression of E-cadherin, a transmembrane protein involved in cell adhesion, and the gain of expression of N-cadherin determines the transition to the vertical-growth phase. From this point, the disease is able to metastasize in distant organs (metastatic melanoma).
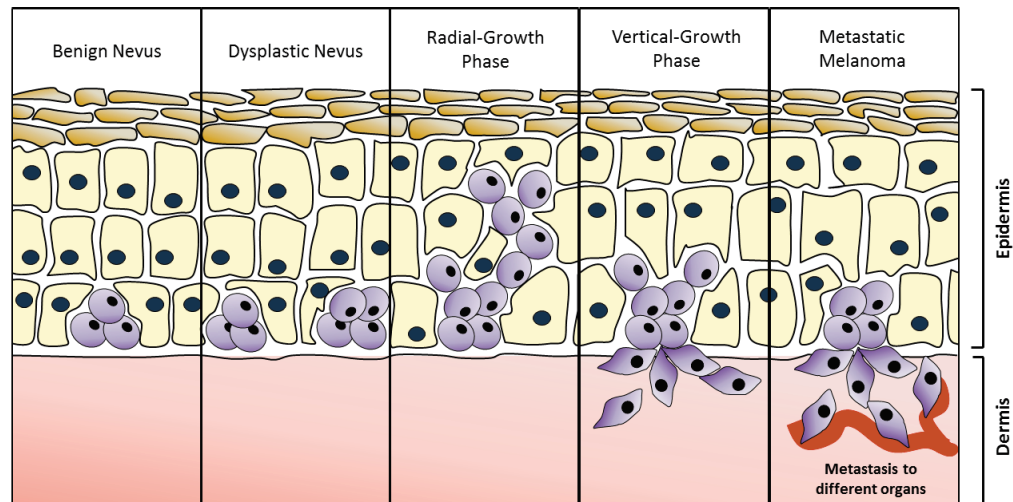
Figure 2. Clark model of melanoma progression. *A benign nevus is represented by a local proliferation of melanocytes. The abnormal proliferation of melanocytes forms a dysplastic nevus, with changes in their phenotype. When cells start to migrate in the nearby epidermis, the melanocytes are in the Radial-Growth phase. If melanocytes start to lose the connection with surrounding keratinocytes and create new contact in the dermis, the vertical growth phase is initiated. The motility of melanoma cells, that can reach different organs, is considered the metastatic phase.*

The **Breslow Depth** is a description of invasion of melanoma in the body, and it is used as a prognostic factor. The thickness of the melanoma is measured with a micrometer from the granular layer of the epidermis down to the deepest point of invasion. This description has been replaced by the American Joint Committee on Cancer (AJCC) staging system.

1.2 STAGING

In order to facilitate the clinical approaches and to improve the outcomes of cutaneous melanoma patients it is fundamental to base the treatment on accurate staging and patient stratification.

Actual melanoma staging is based on the eight edition of American Joint Committee on Cancer (AJCC) staging system, based on the screening of more than 46 000 melanoma patients [6]. The system assigned a stage based on tumor-node-metastasis (TNM) scores, as well as additional prognostic factors.

TNM classification is based on 3 parameters:

- **T**, Tumor, describes the size of the primary tumor
- **N**, Node, describes the presence of cancer cells in lymph nodes regions
- **M**. Metastasis, describes whether the cancer has spread to a different part of the body

In 2009, mitotic rate, expressed as the number of mitoses per square millimeter of primary tumor [7],was added as a criterion to define the stages.

1.2.1 Stage 0 Melanoma – Melanoma *in situ*

Melanoma *in situ* refers to lesions that have breached only the epidermidis (the outer layer of the skin), without growing in the deeper levels and did not show sign of spreading. It is considered a local melanoma. Stage 0 melanoma is highly curable, and patients are considered at low risk for local recurrence or for regional and distant metastases. Surgical excision is sufficient to solve the local melanoma.

1.2.2 Stage I Melanoma

It is possible to divide Stage I into 2 subgroups, influenced by thickness and ulceration status [8], which are strong predictors of prognosis in patients with clinically localized melanomas:

- **Stage IA:** Tumor is < 1 mm thick with or without ulceration when viewed under the microscope
- **Stage IB:** Tumor is ranged between 1mm and 2 mm thickness, without ulceration

_____

1.2.3 Stage II Melanoma

At this stage, melanoma is yet considered a local melanoma (together with stage 0 and stage I), but starts to extend beyond the epidermidis, penetrating the thicker dermis layer of the skin. Pathologic stage II tends to metastasize, but lymph node biopsy results negative.

Stage II is divided into three subgroups:

- **Stage IIA:** Tumor is between 1 and 2 mm thick with ulceration, or between 2 and 4 mm thick but without ulceration,
- **Stage IIB:** Tumor is between 2 and 4 mm thick with ulcerations, or > 4 mm thick without ulceration
- **Stage IIC:** Tumor is > 4 mm thick with ulcerations

1.2.4 Stage III Melanoma

Stage III is also known as "regional melanoma" due to the spreading to nearby lymph nodes, the most common first site of metastasis in melanoma patients [9].

This heterogeneous group is divided into four complex subgroups, based on the number of regional lymph nodes harboring metastatic disease, regional tumor burden and ulceration of the primary tumor.

1.2.5 Stage IV Melanoma

Stage IV melanoma also called "distant metastatic melanoma" has spread throughout the body such as the brain, lungs, liver, gastrointestinal tract or to distant point in the skin. This stage has the poorest prognosis, and the chance of survival 5 year post treatment is less than 10% [9]. Recently, AJCC melanoma staging system introduces three subcategories of stage IV melanoma:

- **Stage M1a**: Metastasis reach distant skin, subcutaneous tissues and/or lymph nodes. Patients at this stage have the highest one-year survival rate (62%) among patients with stage IV disease;

- **Stage M1b**: Metastasis spread to the lungs. Patients at this stage have an intermediate prognosis, with one-year survival rate of 53%;

- **Stage M1c**: Metastasis can be found in any non-pulmonary visceral site or patients with an elevated serum LDH. Patients at this stage have the worst one-year survival among stage IV patients (33%).

1.2.6 The "ABCDE" Rule to identify melanoma

Screening for melanoma has been advocated for many years, due to the fact that early detection and excision have been regarded as the most important measure to lower mortality from neoplasm [10]. The ABCD rule was first introduced in 1985 from Friedman, Rigel and Kopf as a self-diagnosis method that helps people and patients to simply monitoring skin changes, in order to identify lesions that could be potential melanomas. The criteria of identification were: A for "Asymmetry", B for "Border Irregularity", C for "Color Variegation" and D for "Diameter generally greater than 6 mm" [11]. In 2004, the ABCD rule was revisited, adding a new letter that includes any type of change: E for "Enlargement", "Elevation" or "Evolving" [12].

1.2.7 Classification of cutaneous melanoma: the non-acral cutaneous melanoma

Based on clinical and histological features, the primary histologic subtypes of melanoma include superficial spreading, lentigo maligna and nodular. From a genomic standpoint, non-acral cutaneous melanoma (NACM) is generally characterized as being

made up of four major subclasses: BRAF, NRAS, NF1, and triple-wild type.

1.2.7.1 *Superficial Spreading Melanoma*

Superficial melanoma (SSM) constitutes 70% of confirmed melanomas, and generally arises *de novo* or together with an existing nevus. SSM is generally located on the legs of womens and on the backs of men. Its onset is often linked to intermittent sun-exposure as risk factor, as well as family history and Fitzpatrick's phototype I and II, represented by people that in response to UV light are always burn or never tanned (phototype I) or usually burned but with a minimal tan (phototype II) [13], [14]. Histologically, this lesion is characterized by singles or cluster of epithelioid melanocytes, with abundant cytoplasm, nuclear pleomorphism and prominent nucleoli. Pigmentation areas changing from brown to red and sometimes are hypopigmentated. The edges of the lesions are clean and defined, but melanocyte proliferation can be seen extending over 25 mm. Frequently the immunitary response gives rises to spontaneous regression, that clinically appears like a white-grey depigmented area [13].

1.2.7.2 *Nodular Melanoma*

Nodular Melanoma (NM) represents only 5% of melanoma subtypes and is again related to intermittent sun exposure. Differently from SSM, NM is not associated with an existing nevus [13] and presents a rapidly enlarging nodule. NM is generally located on the trunk and limbs of patients ad arise at the age of 50-60 with higher incidence in males [15]. Histologically NM appears generally as a brown mass of dysplastic tumour cells round and epithelioid in morphology with hyperchromatic nuclei.

1.2.7.3 *Lentigo Malignant Melanoma*

Lentigo maligna melanoma (LMM) represents 4 to 15% of cutaneous melanoma, and its onset is related to chronic sun exposed skin with an increased incidence in advanced age. The tumors usually arise from the invasive progression of benign *lentigo maligna*. LMM is usually located in the skin of scalp, face or neck, showing marked solar elastosis and other features of long-term sun damage [13]. Histologically, the lesion presents an irregularly shaped and variable-pigmented macule which slowly enlarges.

1.2.8 Acral Lentiginous Melanoma

Acral Lentiginous melanoma (ALM) is one of the most common variant of melanoma in people with dark skin but arises at equal frequency in all races, mainly arising on the palms, soles and nail beds [16]. Patients with ALM tend to have poor prognosis, mainly caused by delays in diagnosis and advanced disease at presentation [17]. Histologically, ALM may have epithelioid cellular morphology and acanthosis, elongation of rete ridges and extension along sweat ducts are typical features.

1.3 ETIOPATHOLOGY

1.3.1 Incidence

Although malignant melanoma accounts for only about 2% of all cutaneous malignancies, it is responsible for 75% of all skin cancer death. The melanoma incidence and death rate have progressively increased during the last 30 years [18], reaching a global incidence of 15-25 per 100,000 individuals [19], with 48, 000 deaths according to World Health Organization. In 2018, the World Cancer Research Foundation reported 300,000 new cases

worldwide, and 12.1 new cases per 100,000 inhabitants in Italy, ranking 19th among the top 20 nations with highest number of diagnoses. The incidence is influenced by different parameters like ethnicity, geographical location, sex, anatomic distribution and age. Moreover, melanoma incidence is higher in the 40-60 year age group and in later life (> 80 years), and the median age at diagnosis is 57 years [19] Despite this, cutaneous melanoma still remains one of the most common cancers in young adults.

1.4 RISK FACTORS

Many factors that have been considered could affect the increased worldwide incidence of melanoma, and the risk to develop this cancer seems to be linked to genetic, phenotypic, enviromental factors and their combination [20].

1.4.1 Age

Patient age has been considered a strong predictor of outcome, and an independent prognostic factor for survival in patients with cutaneous melanoma [21]. Increasing age is considered an adverse prognostic indicator of overall survival in patients with melanoma, due to unfavourable clinicopathological features in the primary tumor, including thicker depth, higher mitotic rates and increased likelihood ulcerations [21], and epidemiological studies showed that clinical stage I/II patients with more than 70 years had more advanced primary tumors [22] and were associated with higher mortality compared with other age groups [8]. In a correlate study, it was shown how worse prognosis and higher mortality rate in stage III patients was directly correlated with age [23]. However, the causes of heterogeneity of primary melanoma and the diversity of outcomes of the primary melanomas in the young and elderly population have not been clearly defined [21]. Considering age and

anatomic distribution, trunk melanomas occur often in the fith-to-sixth decades of life, while head and neck melanomas occur more in the eigth decade of the life [24].

1.4.2 UV Exposure

Development of melanoma is directly related to UV light exposure, especially UV-B levels, in all skin types [25]: UV radiation cause damage to DNA, playing a pivotal role in the pathogenesis of these tumors. Incidence of melanoma is inversely related to latitude of residence: highest in equatorial regions and less frequent in people who live distant from the equator [26] In this context, epidemiological studies described how sun and time of exposure patterns are directly related with melanoma development. When the skin is exposed to UV light, keratinocytes stimulates melanocytes to produce melanin via UV-induced DNA damage, which induces p53 tumor suppressor protein stabilization [3]. This allow the transcriptional activation of pro-opiomelanocortin, which is cleaved to produce melanocyte-stimulating hormone (MSH) that is subsequently released by keratinocytes to act on melanocytes. Melanocytes respond to the stimulus via Melanocortin 1 receptor (MC1R), that leads to an increasing intracellular level of cAMP, which in turn increases the microphtalmia transcription factor MITF, responsible for melanin synthesis activation [27]. Even if UV radiations could be considered an unavoidable risk factor, the exposure to UV can be strictly controlled. During skin exposure to UV radiation, damaged DNA of keratinocytes stimulates melanocytes to produce melanin, which is packed in melanosomes and transported to keratinocytes, where it protects from UVR-generated free radicals, causing the appearance of tanning [3]. Paradoxically, melanocytes can also be transformed by UVR: in fact, UVR are able to induce genetic changes in the skin but also increase local production of

growth factor and induce reactive oxygen species that can affect skin cells [28]. Oxidative stress can disrupt the homeostasis of melanocytes, compromising their survival or leading to malignant transformation [29]. Even though most melanoma still produce melanin, some damaged melanocytes lose this ability, resulting in a colorless appearance, which makes early diagnosis more challenging [30].

1.4.3 Ethnicity and Geography

The incidence of melanoma seems to be closely related to ethnicity, with a preponderant incidence in the Caucasian population. This variation is probably due to the reduced melanin photoprotection in fair-skinned people, together with variations in UV exposure from intermittent to chronic [31].

Geographic location influence melanoma incidence in people of the same ethnicity [32]. Atmospheric absorption, latitude, altitude cloud cover and season are all variable that influence UV radiation in different geography locations. Lancaster found a correlation between increasing melanoma mortality and closeness to the equator, a phenomenon called "latitude gradient" [32], and from this paper similar trends were recorded over the world, with a higher incidence at higher latitudes.

1.4.4 Sex

Sex influence melanoma incidence differently, and in addition to it, sex incidence is influenced by age. It is reported that adolescent and young women are more susceptible to melanoma compared to men at the same age. Despite this, after the age of 40, the trend reverse, with a higher incidence among men, where the tumor increase more rapidly than any other malignancy [21], [33]. In general, men are most susceptible to melanoma than women, and

the lifetime risk of developing is 1 in 28 for men and 1 in 44 for women [21]. The hypothesis formulated for this difference are formulated basing on behavioural and biological differences the two sexes. Among these, hormonal differences, pharmacokinetics of the drugs and different responses to infection/inflammation [34].

1.5 DRIVER ONCOGENIC MUTATIONS

1.5.1 BRAF

BRAF (V-raf murine sarcoma viral oncogene homolog B1) is a human proto-oncogene, member of the RAF (RApidly growing Fibrosarcoma) family of serine-threonine kinases (ARAF, BRAF and CRAF) with close overlapping functions that constitute part of the RAS/RAF/MEK/ERK mitogen activated protein kinase (MAPK) signal transduction cascade [35], [36].

The study of three-dimensional structure of RAF proteins has played an important role in the characterization of mutations and in the formulation of new drugs act to inhibit its active status. Inactive RAF protein consists in a closed monomeric conformation in the cytoplasm, due to the intramolecular interaction between the carboxyl terminal lobe (C-lobe) and amino terminal lobe (N-lobe) thanks to a flexible hinge (Figure 3 A) [37], [38]. There were identified three major active sites in BRAF: the nucleotide (ATP or ADP)-binding site, the magnesium-binding site (DFG [Asp–Phe–Gly] motif), and the phospho-acceptor site (activation segment [AS]) of the two lobes [39]. In the inactive BRAF (Figure 3A.), the AS is in a helical conformation (called "OUT" position), leading to the positioning of the αC helix. In the "OUT" position ﬛ AS conformation is extended, enabling the αC helix of the N-lobe to flex in the "IN" position, as a light switch (Figure 3B.) [40].
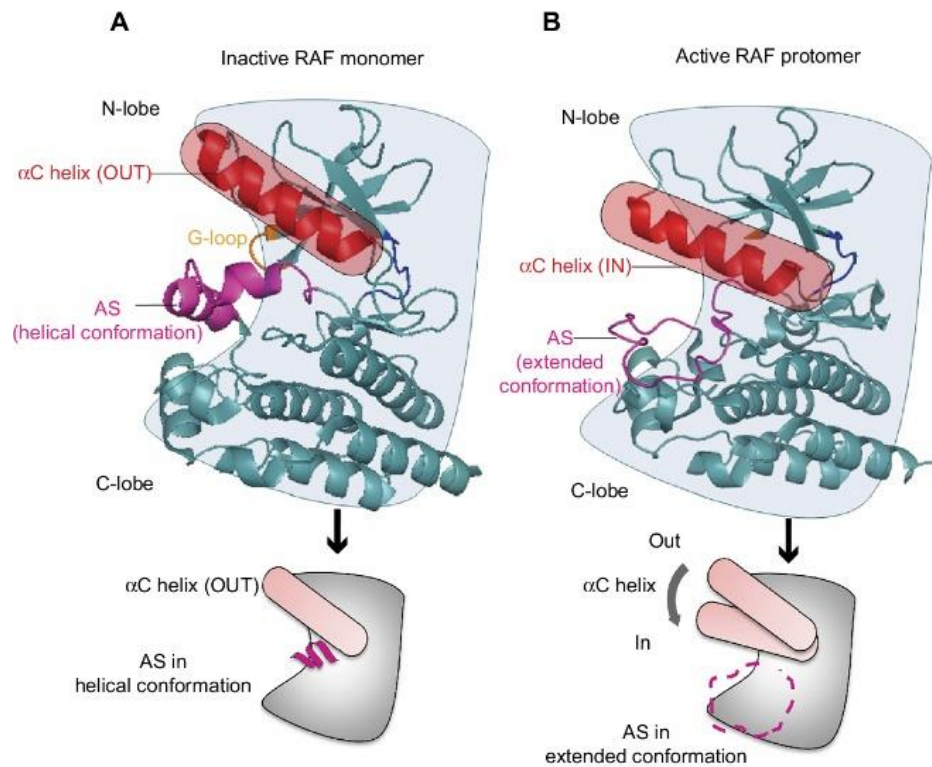
Figure 3. Structural conformation of BRAF. In normal conditions, the inactive monomer (A) own an "OUT" conformation on the active site (AS) had a helical conformation, positioning the αC helix in the "OUT" position. The active form of BRAF (B) is characterized by the extended conformation of the AS, enabling the αC helix to flex in the "IN" position. "Development of small molecule therapeutics and strategies for targeting RAF kinase in BRAF mutant colorectal cancer", Adapted.

Moreover, the DFG "IN" position gives a catalytically competent active conformation [41].

BRAF mutations, firstly characterized in human malignancies in 2002 [42], are present in 5-10% of all human malignancies [43], with a higher incidence in colorectal cancer (10%) [44], papillary thyroid cancer (45%) [45] and malignant melanoma (50%) [43], indicating that this pathway is a key oncogenic driver in multiple anatomic tissues [46]. Moreover, BRAF mutations affect other clinical subtypes of melanoma, representing the 10-20% of mucosal or acral melanoma, while are absent in uveal melanoma [47]. Moreover, BRAF mutations are typically directly related to young age and intermittent sun exposure [48]. The discovery of BRAF-activating mutations in melanoma signed a landmark

_____

event in the understanding of melanoma biology [35]. More than 50 mutations in BRAF have now been described, but 40%-70% of malignant melanoma cases carry a missense mutation, with a substitution of valine with glutamic acid at codon 600 (denoted as V600E). This mutation is located in the activation loop of BRAF [49], and determines a phosphomimetic conformational change in the activation domain of BRAF that leads to a constitutively active MAPK – ERK signalling and a large increase in the basal kinase activity [50]: as a general result, V600E mutation in BRAF destabilize the inactive kinase conformation switching the equilibrium towards the active form, and cells are continuously stimulated to proliferate, while cell death programs are inhibited. Moreover, BRAF[V600E] does not require the dimerization of BRAF for its functions and could act like a monomer. This can result in a 500-fold over-activation of the BRAF kinase cascade [1]. Other driver mutations identified in BRAF are valine-to-lysine (V600K) and valine-to-arginine (V600R) mutations, which comprise 20% and 7% of BRAF mutations, respectively [47]. In a small group of melanoma, BRAF mutations occur in different position than 600, showing impaired intrinsic BRAF kinase activity [51]. It's interesting to notice that about 80% of benign nevi harbor BRAF [V600E] mutations, pointing out how BRAF mutation alone is not sufficient to drive tumorigenesis [42].

Relating BRAF mutations and UV exposure, mutations in BRAF were significantly more frequent in melanomas of patients without chronic sun exposure [52].

1.5.2 NRAS

With 15-20% of cases, NRAS mutations at codons 12, 13 and 61 constitute the second most common genetic alteration in non-uveal sites melanoma, and are associated with increased aggressiveness

and poor survival [42]. BRAF and NRAS mutations are always mutually exclusive [47] and differently from BRAF, NRAS mutation is rare in benign melanocytic nevi [53]; however, NRAS play an important role in resistance to target therapy with BRAF inhibitors.

NRAS tumors tend to arise in the later-life (> 55 years), and are correlated with chronic ultraviolet (UV) exposure in contrast with BRAF-mutated tumor that are more common in intermittently sun-exposed skin [54].

The presence of NRAS mutations is also considered an adverse prognostic factor in melanoma, tending to be more aggressive than other subtypes with thicker lesions, elevated mitotic activity and higher spreading of metastasis to the lymph nodes; people who harbor this mutation has a lower median OS compared to non-NRAS-mutant melanoma [55].

Moreover, and in contrast with BRAF-mutant melanoma, little progress has been made in developing targeted therapeutic strategies for NRAS-mutant melanoma; no effective small-molecule inhibitors have been detected.

1.5.3 Loss of NF1

The neurofibromin 1 (NF1) gene located on chromosome 17, encodes for a protein that works as a negative regulator of RAS signal transduction pathway. In basal conditions, NF1 function is a GTPase-activating protein known to downregulate RAS activity by converting the active RAS-guanosine triphosphate (RAS-GTP) into the inactive form RAS-guanosine diphosphate (RAS-GDP) [56]. As a result, RAS/MAPK pathway results negatively regulated [57]. NF1 mutations are common in cancer (i.e. neurofibromas, plexiform neurofibromas, myeloid leukemia and Lysh nodules,, and affect approximately 12-18% of all melanoma

_____

[57]. Furthermore, desmoplastic melanoma, a rare form of cancer, shows a loss-of-function mutation in NF1 in more than 50% of patients [58]. The major consequence of loss of NF1 mutation is an increasing in RAS/MAPK pathway signaling. Moreover, NF1 seems to play a role in driving resistance to RAF/MEK targeted therapies [56]. NF1 mutations occur in melanoma patients after chronic skin sun-exposure or in older individuals. Genome Atlas Network and Krauthammer et al. [59] point out that mutation in BRAF or in RAS may also have a loss-of-function in NF1.

1.5.4 Triple Wild Type Melanoma

Triple Wild-Type subtype melanoma is an heterogeneous subgroup characterized by a lack of hot-spot BRAF, N/H/K RAS or NF1 mutations [57], and a higher fraction of samples possess significant copy amplifications in the 4q12 minimal common region containing v-kit Hardy-Zuckerman 4 feline sarcoma viral oncogene homolog (KIT), platelet derived growth factor alpha (PDGFRA) and kinase insert domain receptor (KDR, VEGFR2), as well as amplifications in loci encompassing telomerase reverse transcriptase (TERT), cyclin dependent kinase 4 (CDK4) and cyclin D1 (CCND1) [60] (Figure 4). Only 30% of cases harbored a UV signature, compared to over 90% for the other three categories [57]. Triple wild type melanomas were frequently observed in males between the age of 60-70 [61].
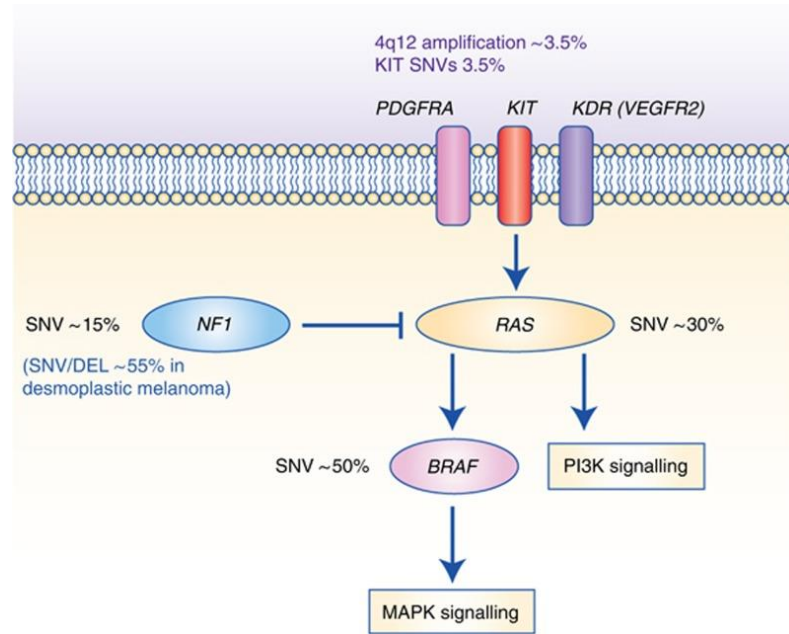
Figure 4 Schematic representation of oncogenic mutations in melanomas. *Among the most studied oncogenic mutations is it possible to find BRAF, NRAS, loss of NF1 and Triple Wild Type melanoma. All these mutations are involved in proliferation and survival pathways.*

1.6 THERAPEUTIC APPROACH

Food and Drug Administration (FDA) approved several therapies over the past years. Therapeutic options depend on location, genetic profile and stage upon the diagnosis.

Therapeutic options may be surgical resection, chemotherapy, radiotherapy, photodynamic therapy (PDT), immunotherapy or targeted therapy [62].

1.6.1 Surgery

Currently surgical excision is still the first approach for patients with the early stage disease (Stage I-IIIB), with different procedures depending on clinic-pathologic features of the tumor [62]. The resection of the lesion is generally associated with an excellent prognosis [63]. Primary metastatic melanoma is also treated with surgery alone [64], while in patients above stage IIIB surgery is no longer sufficient and becomes more difficult to treat,

needing adjuvants systemic treatments to limits melanoma from recurring or spreading.

1.6.2 Radiotherapy and Photodynamic therapy (PDT)

Radiotherapy is considered the most effective non-surgical mode of locoregional therapy of melanoma, also suitable as adjuvant therapy after a complete excision of primary melanoma in order to reduce the rate of local or nodal recurrence, or as palliative treatment option in case of advanced or disseminated disease [65]. Sometimes, radiotherapy is also used in case of unsuitable major surgery or in case of refuse proposed surgical intervention [65].

Photodynamic therapy (PDT) is an effective treatment for several cancers (REF) and consists that in a combination of a systemic or local administration of photosensitizers dyes (i.e. hypericin, benzoporphyrin derivatives, protoporphyrin IX) in combination with an activating irradiation with a specific wavelength in presence of oxygen, generate short-lived reactive oxygen species (ROS) [66]. ROS generated by the treatment are responsible for the selective tumor destruction, tumor-associated vascular damage and activation of immune responses [67].

1.6.3 Chemotherapy

Chemotherapy represents the first approved treatment option for advanced melanoma. Anti-tumor effects were obtained with Dacarbazine, platinum analogs and nitrosureas (Brahmer JR, Phase I study of a single-agent anti-programmed death-1 immunologic correlates). The alkylating agent Dacarbazin was approved in 1974 by FDA, and used as standard chemotherapy medication. The effectiveness of this chemoterapeutic agent has been validated for several years, but only 7.5% of patients respond to therapy.

Unfortunately, the single agent or synergistic treatments with immunotherapy or biologic agents did not improve the overall survival (OS) of patients, probably due to development of drug resistance [31].

1.6.4 Immunotherapy

Cancer cells and immune system are closely related, and it is known that the appearance of tumors is often associated to presence of chronic inflammation site and infiltration of immune cells in the tissues. Moreover, melanoma is considered a particularly immuno-genic tumor, making immunotherapy of melanoma a dynamic field of research [31].

In 1995, interferon alpha 2-beta was the first immunotherapy approved by FDA as an adjuvant therapy for stage IIB/III melanoma [68] and at present, it persists in clinical trials in combination with targeted therapies [62]. In these cells, IFN-alpha shows an immunomodulatory dose-dependent anti-proliferative effect, stimulating major histocompatibility complex class I expression of melanoma [62]. On one hand, high-dose adjuvant IFN-alpha reduces the risk of recurrence in melanoma patients [69]. On the other, only a small percentage of patients respond to IFNs adjuvant treatments.

Like IFNs, interleukin-2 (IL-2) is still included in clinical trials as an adjuvant therapy of chemotherapy, radiotherapy or targeted therapy for metastatic melanoma. This cytokine is able to expand effector T-cells (Teffs) and Treg populations [70], being able to inhibit proliferation of melanoma cells. Moreover, Joseph R.W et al showed in their retrospective study that patients with NRAS mutations better respond to high dose IL-2 therapy [71].

Ipilimumab is a fully human monoclonal anti-CTLA-4 antibody, approved for the treatment of unresectable or metastatic

melanoma [72] and is one of the first drugs that showed survival benefits in this patients. Ipilimumab is able to block CTLA-4, an inhibitory checkpoint receptor that blocks T-cell activation and induces immune tolerance [62]. Blocking the inhibitory action of CTLA-4, Ipilimumab enhance T-cell responses, resulting in an higher pro-inflammatory T-cell cytokine production, and better T-cell responses to tumor antigens, resulting in immune-mediated antitumor activity with an increasing T-cell expansion and infiltration in responding tumors [73].

Other interesting approaches based on immunotherapy are the oncolytic virus and peptide vaccines.

1.6.5 Targeted therapy

Alternatively to cytostatic chemotherapy, the new concept of cancer therapy is focused on targeting mutated proteins that may control cell proliferation and malignant phenotype [62]. The approach uses small molecule inhibitors or antibodies that affect these mutated proteins, involved in the progression of the disease. Moreover, the advantage of the targeted therapy is the possibility of selecting the patients who will benefit from the treatment, based on the mutational profile of the tumor [62]. Interestingly, the identification of oncogenic driver mutations in human cancer, such as KRAS and BRAF, has accelerated the development of small-molecule inhibitors along the RAS-RAF-MEK-MAPK signalling pathway [46].

Vemurafenib offers a novel, first-line, personalized therapy for patients who have mutated BRAF.

1.6.5.1 *Vemurafenib*

Vemurafenib (chemical name: propane-1-sulfonic acid {3-[5-(4-chlorophenyl)-1H-pyrrolo[2,3-b]pyridine-3-carbonyl]-2,4-

difluorophenyl}-amide; Commercial name Zelboraf, PLX4032) (Figure 6) is an orally bioavailable molecule with a low-molecular-weight (489.93 Da), firstly synthetized in 2005 by Plexxikon (with the name of PLX4072) and reformulated through F. Hoffmann-LaRoche (Basel, Switzerland) collaboration and approved by FDA in 2011 for the treatment of advanced BRAF^{V600E}-positive metastatic melanoma [74], [75]. This BRAF-specific inhibitor compound is highly effective in cells with BRAF^{V600E} mutation rather than the wild type, thanks to the selective binding to the ATP-binding pocket of the constitutively active form of BRAF mutated. In particular, based on the structural features of the αC helix and DFG position in BRAF, this molecule belongs to the type$_{1/2}$ category of structural type inhibitors: PLX4032 is able to
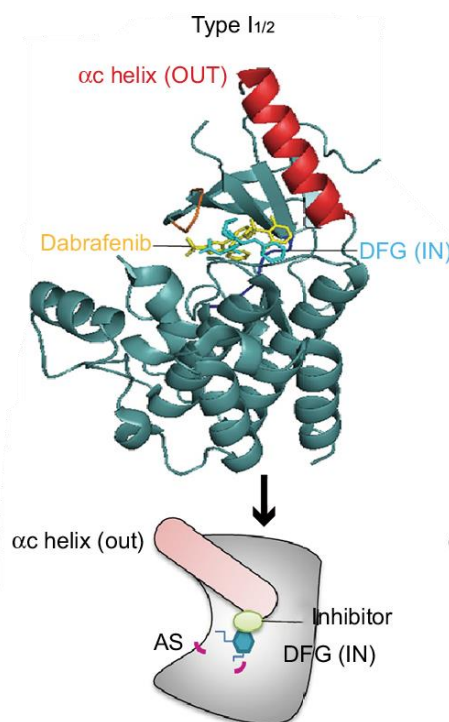

***Figure 5**. **PLX4032 positioning on BRAF.** Type$_{1/2}$ inhibitors is able to bind to the DFG "IN" position, stabilizing the αC helix in the "OUT" position. "Development of small molecule therapeutics and strategies for targeting RAF kinase in BRAF mutant colorectal cancer", Adapted.*

_____

bind to the active site of the kinase domain in the "DFG-in" motif conformation (stabilized by V600E mutation), blocking the access of ATP and stabilizing the αC helix in the "OUT" position (Figure 5) [76] [49], [77].

Co-cristallography studies of BRAF^{V600E} with Vemurafenib revealed that the homologue PLX4032 is able to bind to one of the two BRAF promoters with 100% occupancy while the other promoter that is only 60% occupied by PLX4032, needs to adopt the DFG-out conformation, so as to interfere with the BRAF dimerization as a final effect [49]. The biochemical affinity of Vemurafenib for the mutated BRAF translates into potent inhibition of ERK phosphorylation only in BRAF-mutant cell lines, causing the arrest of the cell cycle and apoptosis in vitro, and a regression of the tumor growth in vivo [78]. In the phase I clinical trial, 80% of patients carrying the BRAF^{V600E} mutation respond to PLX4032 therapy. The recommended dose of PLX4072 in clinical setting is 960 mg orally twice daily with a mean maximum concentration (Cmax) reached in the blood of 4.8 ± 3.3 μg/ml and an inhibitory concentration of 50% at 31 nmol/L [79]). PLX4072 requires 4 hrs to reach the maximum concentration after absorption (tmax) while the mean half-life (t ½) is 57 hrs [79], resulting in six to nine-fold accumulation between Day 1 and Day 15 [78]. The molecule is excreted via faeces (94%) and urine (1%), with a clearance of approximately 30 L/day [75], [80]–[82].

Pharmacodinamical studies on pre- and post- treatment paired biopsies shows that the clinical activity of PLX4032 is effective when BRAF is inhibited at a level of more than 80%. Moreover, it was noticed that the inhibition of cytoplasmic pERK levels, but not inhibition of nuclear pERK levels, correlate well with tumor response [35], [83]. Compared to Dacarbazin chemotherapy, PLX4072 is able to reduce in a phase 3 trial the relative risk of

overall and progression-free survival by 63% and 74%, respectively, in 675 treatment-naïve patients with the BRAF[V600E] mutation [84], extending melanoma survival from 4 to 6 months [46]
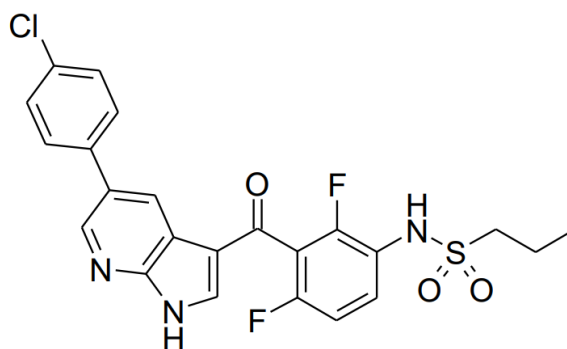
Figure 6. Chemical Structure of Vemurafenib.

1.6.5.2 *Other BRAF inhibitors*

Dabrafenib (GSK2118436I) is another potent selective BRAF inhibitor, active towards BRAF[V600E] and also against non-melanoma V600E BRAF-mutant cancers, including papillary thyroid, colorectal, ovarian. FDA approved clinical Dabrafenib treatment in 2013 for metastatic melanoma patients with brain metastasis [85]. Resistance to Dabrafenib occurrs after 6 to 7 months from the treatment: for this reason, drug combination with MEK inhibitor Trametinib plus Dabrafenib is used in therapy [86]. Sorafenib (BAY 43-9006, Nexavar) is an orally available multi-kinase inhibitor including wild type and V600E mutant BRAF [87], [88]. Moreover, this compound is able to inhibit vascular endothelial growth factor receptor VEGFR1, VEGFR2, VEGFR3 and platelet-derived growth factor receptor (PDGFR-beta) [88]. Initially approved for the treatment of primary kidney cancer and advanced primary liver cancer. Sorafenib as single agent therapy

in melanoma metastatic treatment did not show significant results.

1.6.6 Resistance towards BRAF inhibitors

Despite the encouraging results obtained with Vemurafenib treatments, most of the BRAF-mutant metastatic melanoma patients after 6/7 months no longer respond to therapy, and relapse. Long-term efficacy is thwarted due to emergence of tumor resistance, the principal factor for the failure of cancer therapy [89]. Cancer cells can become resistant under selective pressure of therapies (intrinsic resistance), due to the presence of preexisting resistant clones, or should be secondary resistant due to an evolving process during the treatment (acquired resistance) [47].

Due to the extreme heterogeneity of this tumor, melanoma could acquire new mutations or epigenetic modifications during the passage from primary lesion to metastases [90]: as a result, in the same patient can coexist cells with susceptible $BRAF^{V600E}$ mutations together with cells that may carry different mutations not susceptible to BRAF inhibitions. The variety of resistance patterns found in individual tumors point out that each individual own complex defence mechanisms against toxic substances creates a unique resistant profile [89].

1.6.6.1 *Acquired Resistance*

Despite the great advances in melanoma therapy thanks to BRAF inhibitors, a significant proportion of $BRAF^{V600E}$ mutated melanoma does not respond to therapy, showing signs of drug resistance [35].

_____
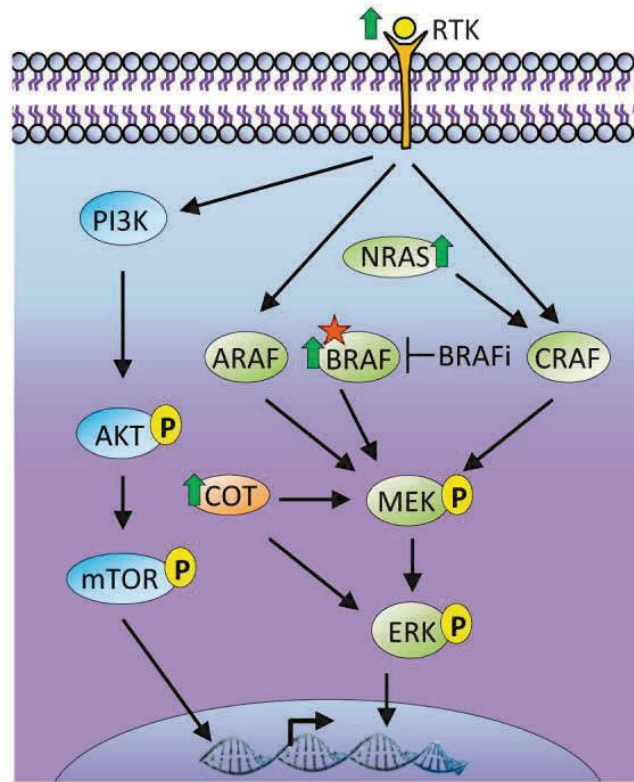
Figure 7. Acquired resistance mechanisms in BRAFV600E mutated melanoma, treated with BRAF inhibitors. *Acquired resistance in melanoma could be due to several mechanisms. Among these: reactivation of MAPK/ERK pathway downstream, upstream or at BRAF level; activation of MAPK/ERK through different isoforms of RAF protein; the activation of alternative pathways such as PI3K/AKT or COT.*

Acquired resistance is usually due to the reactivation of upstream or downstream MAPK signalling pathway [91] or the reactivation of BRAF; otherwise it could be due to the activation of alternative signalling cascade like PI3K/AKT [92], or enhanced activity of Tirosine-Kinase Receptor (RTK) [93] (Figure 7). Notably, in case of acquired resistance no secondary mutations on BRAF[V600E] were found [94]. However, alternative splicing of BRAF[V600E] or copy number amplification were identified, resulting in strong reactivation of MEK and ERK, even in the presence of a BRAF inhibitor [95].

When BRAF is blocked, ARAF and CRAF isoform could reactivate the ERK signalling pathway [96] through RAS activation,

_____

allowing the proliferation and acting as an alternative survival route.

Through the ERK negative loop, BRAF^{V600E} could partially restore its activity: the blockage of BRAF by inhibitors relieves ERK negative feedback on RAS, partially restoring RAS activity. This determines BRAF^{V600E} dimerization; the binding of PLX4032 on one of the two component of each dimer transactivates the other unbound component, partially restoring the ERK pathway [97].

Moreover, RAS mutations can allow proliferation: when RAS is mutated, RAS-GTP cannot return to its inactive GDP-bound state, becoming constitutively active. This enhances BRAF^{V600E} dimerization and confers resistance to the drug [98], [99].

Downstream, mutation on MEK1/MEK2 can overcome BRAF inhibition [93].

The reactivation of BRAF^{V600E} is mainly due to the amplification of the mutant BRAF allele [100] : consequently, BRAF resulted overexpressed. Moreover, the amplification of BRAF promotes BRAF^{V600E} dimerization. In both cases, MAPK/ERK resulted reactivated, and BRAF inhibitors cannot compensate the increased BRAF expression [100].

Due to some points of interaction between MAPK/ERK and PI3K/AKT pathways, PI3K/AKT upregulation can work as a compensatory mechanism that can overcome BRAF inhibition and drive resistance [101], stimulating anti-apoptotic signals and increasing expression of key proliferative genes. Mutations on PI3K/AKT have been identified on 22% of melanomas with acquired resistance to BRAF inhibition [94].

Furthermore, PI3K/AKT pathway is activated by the binding of growth factors (i.e. PDGFß and IGF-1R) to RTKs. The

upregulation of these receptor when BRAF is inhibited leads to a persistent PI3K/AKT signalling.

PTEN negative or high basal PI3K/AKT signalling are predictive signals of resistance to targeted therapy agents, showing a marked impairment of therapy-induced apoptosis and poor therapeutic responses [35].

1.6.6.2 *Intrinsic resistance*

It is well established that BRAF^{V600E} amplification was sufficient to overcome BRAF inhibition in 20% of cases [100] describing these patients as intrinsic resistant to BRAF inhibition [93].

The intrinsic resistance of melanoma to BRAF inhibition has been linked to mutations on different genes, that could also be related to the onset of acquired resistance [102]. Some of these genes are already classified as melanoma oncogenic drivers, i.e. loss of NF1, previously described in this thesis. Among the most studied genes is it possible to find loss of phosphatase and tensin homolog (PTEN), amplification of cyclin D1 (CCND1), and MAP3K8 overexpression [93].

Loss of PTEN is considered one of the most frequent mutation responsible for intrinsic resistance, which occurs in 35% of cases [47]. PTEN is a tumor suppressor, negative regulator of PI3K: the loss of its function in patient treated with BRAF inhibitors determines a constitutive activation of PI3K/AKT pathway, leading to cellular proliferation, growth and survival [103].

Upregulation of Cell cycle regulator Cyclin D1, encoded by CCND1 gene, allow cells to grow without needing BRAF pathway activation [93].

Intrinsic resistance is also related to an overexpression of MAP3K8, a gene that encodes for cancer Osaka thyroid oncogene (COT), able to independently activate the MAPK/ERK pathway

[104]. For this reason patients that intrinsically overexpress COT who are exposed to BRAF inhibitors, molecularly respond by producing an excess of COT, slowing cellular proliferation. This was confirmed by a study of Johannesen CM et al, that evidence that low BRAF[V600E] levels correlate with increased levels of COT [104].

1.7 THE MAPK SIGNALING PATHWAY

The RAS-RAF-MEK-ERK mitogen-activated protein kinases (MAPK) pathway is an evolutionarily conserved Ser/Thr kinases cascade that acts like a signal transducer able to convert extracellular stimuli into nuclear (cellular) responses [105] such as growth, proliferation, differentiation, migration and apoptosis. The pathway is composed by a regulatory small G protein (RAS) and a three-tier consequently phosphorylated kinases module (RAF-MEK-ERK). The binding of a ligand (e.g. growth factors, hormones or cytokines) on the extracellular portion of a transmembrane tyrosine kinase receptor (RTK) is the starting point of the signalling cascade. Active RAS acts via adaptor protein to activate and recruit RAF proteins to the cell membrane where they are activated [1]. As a result, the conformational changes in RAF activate the MEK1/2 and ERK 1/2 phosphorylation cascade until the translocation of phosphorylated ERK to the nucleus, where it is able to activate transcription factors that regulate expression of genes involved in cell growth, proliferation and survival [106]. Abnormalities in MAPK signalling helps cancer cells to acquire needful capabilities such as independence of proliferation signals, evasion of apoptosis, insensitivity to anti-growth signals, unlimited replicative potential, ability to invade and metastasize, attract and sustain

angiogenesis for nutrient supply [107] and also acquire drug resistance and avoid oncogene induced senescence [108].

1.8 MITF

Microphtalmia-associated transcription factor (MITF) is an evolutionary conserved DNA binding protein that belongs to the MiTF/TFE transcription factor family. All the members of this family share a common basic helix-loop-helix leucine zipper (bHLH-LZ) motif that allows to bind DNA on E-Box (CACGTG) and M-Box sequences and regulates the transcription of target genes involved in a wide range of cellular processes such as differentiation, proliferation, migration and senescence [109], and recently its function has been recognized also in the regulation of energy metabolism and organelle biogenesis [110]. Functionally, MITF binds to DNA as a dimer and it is also able to heterodimerize with other transcription factors member of MITF/TFE family such as EB (TFEB), TFE3 and TFEC [111].

MITF is a result of differential splicing and multi-promoter usage, giving rise to specific isoforms that differ in their first one or two exons. Some of these isoforms are tissue-restricted, suggesting that MITF could activate a specific subset of genes in a tissue-specific manner [112]. MITF-M is the isoform specifically expressed in melanocytes, and it is considered the "master regulator of melanocyte biology", due to its importance in melanocyte development from the neural-crest and for the signalling [112]. Although MITF represents a lineage-restricted regulator that operates in normal cells, its activity is also important in the molecular mechanisms of malignant cells, and its role as melanoma addiction oncogene was hypothesized [110]. The regulation of MITF-M promoter is subjected to the activation of different transcription factor including paired box gene 3 (PAX3),

cAMP-responsive elements binding protein (CREB), SRY (sex-determining region Y)-box 10 (SOX10), lymphoid enhancer-binding factor 1 (LEF1, also known as TCF), one cut domain 2 (ONECUT-2) and MITF itself [112]. MITF is able to operate within a wide range of activity levels determining melanoma cell fate: high activity of MITF is related to differentiation or proliferation mechanisms while low activity of MITF is typical in stem cell-like or invasive potential [110] but also with cell senescence. However, evidence for the role of changes in MITF levels in melanoma is contradictory: in fact, high expression of MITF was found in melanoma relapse after combined BRAF and MEK inhibitor therapy [113], but resistance to targeted therapy has also been associated with a decrease expression of MITF [114]. This versatility highlights the central regulatory role of MITF in melanoma cell phenotype.

1.9 METABOLIC PATHWAY

1.9.1 An overview of Central Carbon Metabolic Pathway

Central Carbon Metabolism consists of glycolysis, the pentose phosphate pathway (PPP), and tricarboxylic acid (TCA) cycle [115].

In order to survive and to proliferate, cells needs to provide to their energy requirements imposed by vital processes. Normoxic, nonmalignant cells primarily rely on mitochondrial oxidative phosphorylation to generate the energy needed for cellular processes [116]. In presence of oxygen, a molecule of glucose is broken down in the cytosol through glycolysis in two molecules of pyruvate: after mitochondria internalisation, decarboxylation of pyruvate by mitochondrial pyruvate dehydrogenase (PDH) initiates the highly efficient process of mitochondrial oxidative phosphorylation (OXPHOS) [116] and the production of acetyl-

_____

CoA feeds the tricarboxylic acid (TCA) cycle. Successive oxidation of acetyl-CoA into TCA cycle leads to transfer electrons to NAD+ to produce NADH, which in turn is consumed by oxygen-dependent reactions producing carbon dioxide (CO_2) and water (H_2O). Moreover, NADH transfer electrons to the electron transport chain (ETC). The transportation of protons through the mitochondrial membrane is the fuel needed to generate ATP from ADP, finally producing 36 molecules of ATP, with oxygen serving as the final electron acceptor and producing water and a small amount of lactate as by-products. TCA cycle and OXPHOS is a highly efficient chemical energy conversion pathway [46], but in tumor mass cells rely more on less efficient glycolysis to meet their energy needs [115].

1.9.2 Glycolysis and OXPHOS in cancer cell metabolism

In order to survive and proliferate, melanoma cells increase the glucose uptake and mostly metabolize it into lactate regardless oxygen levels, a process known as "aerobic glycolysis" or "Warburg effect" in honor of Otto Warburg, who first described the propensity of tumor cells to utilize glycolysis [117]. It was shown from Scott et al that in normoxic conditions, only 25% of pyruvate enters the mitochondria of melanoma cells exhibiting the Warburg phenotype, where it is converted in Acetyl-CoA by pyruvate-dehydrogenase (PDH) [117]. Warburg phenotype and metabolic reprogramming is also driven in part by activation of molecular signaling pathways, including MAPK pathway. Its activation causes the transcription of hypoxia inducible factor 1 alpha (HIF-1 alpha) and stabilizing the interaction with HIF1beta. This bond promotes glycoyisis via transcription of LDH, aldolase and enolase I.

Despite the evidence which supports the Warburg hypothesis, it is also necessary to consider tumor as a dynamic system, subject to continuous modification in response to enviromental stresses: this includes that metabolic networks change constantly to adapt cancer cell to external signals, in order to survive.

It is known that various cancer cells are strongly addicted to other carbon sources such as glutamine or fatty acids: these molecules are oxidized by mitochondria to produce energy and/or anabolism, adding a mitochondrial oxidative phenotype as an alternative to glycolytic phenotype [118]. OXPHOS is a fundamental pathway required for the growth of different cancers like leukemias, prostate, breast cancer and also melanoma [46]. Barbi de Moura et al showed through bioenergetics analysis that metastatic melanoma in vitro had an high level of OXPHOS in addition to glycolysis [119].

1.9.3 Lactate production and its importance in melanoma metabolism

Lactate is the end product of glycolytic pathway, in order to maintain NAD^+, lactate is secreted from the cell primarily through monocarboxylate transporters (MCTs), with MCT4 as the most significant transporter.

It was demonstrated that a higher expression of GLUT1 and MCT4 transporters are closely related to tumor progression, pointing out that Warburg Phenotype and lactate secretion cooperate to promote melanoma metastasis [120]. The release of lactate into the tumor microenviroment (TME) determines drastic alterations facilitating angiogenesis, promoting metastasis and suppressing immune system [115], and the release of protons produced via dissociation of lactic acid contributes to lower the pH of extracellular space [115]. The acidification of pH is also due to

additional membrane protein complexes like carbonic anhydrase IX (CAIX), sodium-bicarbonate transporter 1, and anion exchanger 2 (AE2).

1.9.4 MAPK/ERK pathway and metabolism

Oncogenic mutation largely contributes to the reprogrammation of the metabolic profile that influences cancer cell fate, sustaining cell survival and proliferation regardless external conditions. Some of these were identified in melanoma, including BRAF, NRAS, KIT, GNAQ, GNA11, NF1 and telomerase [121], and most of them, including are able to activate MAPK/ERK pathway.

In the context of BRAF-MEK-ERK signalling, mutant BRAF exhibits an increased expression of glucose transporters as well as glycolytic genes, resulting in a glycolytic phenotype with inhibition of oxidative phosphorylation [118], [122]. Cellular reprogramming through BRAF^{V600E} overexpression causes modification in the expression of numerous metabolic genes, such an increasing in lactate dehydrogenase A (LDHA) and pentose phosphate pathway enzymes [50]. This evidence indicates that glucose metabolism could be important for BRAF-driven tumorigenesis.

1.9.5 BRAF inhibitors and metabolism

The metabolic effect of the inhibition of MAPK pathway in tumor cells is the reduction in glucose utilization and in the glycolytic flux, resulting from the regulation of the glycolytic regulator HIF1α and MYC.

Moreover, it is demonstrated that BRAF^{V600E} inhibition is able to suppress uptake of radioactive glucose tracer 2[18F]fluoro-2-deoxy-d-glucose (FDG) in BRAFV600 human melanoma cells and xenografts [123] and in patients with BRAF^{V600E} melanoma,

suggesting that the inhibition of glycolysis could be important for clinical response to BRAFi [124].

2 AIM OF THE WORK

Understanding cancer relapse development requires an indepth-study of the processes underlying cancer drug resistance. The causes behind this phenomenon are multi-fold and often include different mechanisms including drug efflux, target alteration, drug degradation, epithelial mesenchymal transition, immune system evasion and enhanced or alternative metabolism [125]. Moreover, the development of drug-resistant tumors further modifies the phenotypic behavior of cancer. This is also made more complex by the heterogeneity of the patient's response to the therapy, highlighting the need to find personalized therapies based on the pattern of patient's specific tumor.

Among the latest therapeutic strategies adopted for the treatment of tumors, it is possible to find target molecules which focus on targeting mutated proteins in order to shut down specific altered pathways. However, the problem arises when cancer cells express a pattern of resistance mechanisms able to constitutively activate oncogenes which can support cell survival [125]. In this regard, BRAF^{V600E} mutated melanomas show a constitutive activation of the MAPK pathway cascade that promotes cell growth [126]. Patients with unresectable metastatic BRAF^{V600E} tumors are treated with BRAF^{V600E} inhibitors (Vemurafenib, Dabrafenib), alone or in combination with MEK-ERK inhibitors (Trametib), in order to switch off the survival pathway. Despite this pathway being a target-model for selective therapy, the tumor is able to overcome BRAF inhibition through the reactivation of the MEK-ERK cascade or the upregulation of alternative signalling

pathways. Although the tumor initially responds to BRAF^{V600E} inhibitors, the use of the drug progressively decreases the tumor dependence on the pathway, and the chronic treatment with the inhibitor determines the activation of alternative pathways, also in combination with other drugs.

However, the clinical response of patients to the treatments is not unique, so it is crucial to identify the specific features that can predict the effectiveness of the treatment on the subset of patients. According to the principle of personalized medicine, based on the identification of specific markers and mutations that allow the formulation of increasingly effective therapies [127], it is necessary to improve the *in vitro* models in order to obtain more information on the *in vivo* different responses.

In order to overcome drug resistance and design personalized therapy, it is important to better identify the heterogeneous survival mechanisms directly using experimental models that can reflect clinical conditions and tumor responses. In this context, our research group selected a multi-drug resistant model of a human MYCN-amplified neuroblastoma (NB) cell line in order to investigate the molecular mechanisms responsible for Etoposide resistance [128]. In this previous study, NB-resistant cells, after chronic treatment with Etoposide, were shown to have a major oxygen consumption and an increased oxidative phosphorylation in respect to the non-resistant counterparts. Based on these findings, understanding the role of metabolism in drug-resistance is crucial to establish a therapeutic approach in cancer treatment.

In the current thesis, the main aim was to select a human metastatic melanoma BRAF^{V600E} mutated cell line after a long-term treatment with PLX4032 in order to obtain an in vitro model for studying the mechanisms of PLX resistance. Herein, the

phenotypic changes and the metabolism of this PLX-resistant melanoma cell line were investigated to identify "metabolic strengths" that must have taken into account to fight melanoma malignancy and relapse.

3   MATERIAL AND METHODS

3.1   MODEL SYSTEMS

3.1.1   Cell lines

All the experiments in this thesis have been performed using a human cell line, derived from patient biopsies, growing as two-dimensional mono-cultures. Optimization of cell densities was performed for all test conditions, since over-confluent cell cultures can lead to underestimation of cell proliferation, signaling and drug efficacy [129], [130].

In detail, MeOV Human melanoma cell line was kindly donated from Dr. Gabriella Pietra (University of Genoa, Genoa, Italy), established directly from the biopsies of an untreated patient and maintained in RPMI 1640 medium supplemented with 10% Fetal Bovine Serum (FBS, Euroclone Spa, Pavia, Italy), 1% L-Glutamine (Euroclone) and 1% Penicillin/Streptomicin (Euroclone) and grown in standard conditions (37°C humidified incubator with 5% CO_2).

3.1.2   Generation of chemo-resistant subclones and certification of autenthicity of the lines

The MeOV PLX-Resistant (PLX-R) and dimethyl sulfoxide - Resistant (DMSO-R) subclones were gradually selected by treating MeOV cell line with increasing concentrations of PLX4032 (Selleckchem, Texas) or DMSO, used to solve PLX, as control. The DMSO-R subclone is PLX-Sensitive, and it is used as a comparative model in order to exclude a toxic effect of DMSO chronic treatment, and a potential interference with the effects exerted by PLX chronic exposure.

In details, sub-confluent cells were initially treated with 250 nM of the drug for 72 hrs. Then, drug was removed and cells were allowed to recover (according to [131], this procedure is defined as

"recovery time" of this cell line). Upon recovery, cells were again treated with the same concentration of the drug for 3 times, before increasing the concentration of the drug. This process was repeated for a period of 6 months, to generate resistant cell lines, reaching the concentration of 1.5 µM PLX and 0.0075% v/v DMSO. The culture medium was changed once a week and cells were seeded at 1.5×10^6 density twice a week.

To certify the authenticity of these lines, Short Tandem Repeat (STR) profile of MeOV DMSO-R and PLX-R was carried out by U.O. Service of Immunoematology and Trasfusional, Ospedale Policlinico San Martino. Fifteen highly polymorphic STR loci plus amelogenin (Cell ID™ System, Promega, Milan), were used. Detection of amplified fragments was obtained by ABI PRISM 3100 Genetic Analyzer. Data analysis was performed by GeneMapper® Software version 4.0 (Thermo Fisher Scientific, Waltham, MA, USA),

3.1.3 Treatments

MeOV PLX-R and DMSO-R cells were treated with 1.5 µM of PLX4032, (Selleckem) or 0.0075% v/v DMSO (Santa Cruz) for 24, 48 and/or 72 hrs, depending on the experiment. Cell cultures were carefully inspected before and during the experiments to be sure that cell density was optimal (samples were discarded if cell confluence reached > 90%).

3.2 EXPERIMENTAL PROCEDURES

3.2.1 Cell Viability (MTS) Assay

In order to test cell viability, 3-(4,5-dimethylthiazol-2-yl)-5-(3-carboxymethoxyphenyl)-2-(4-sulfophenyl)-2H-tetrazolium (MTS) CellTiter 96 Acqueous One Solution Cell Proliferation Assay

system (Promega) was performed according to the manufacturer's instructions.

MTS is able to measure the activity of living cells via mitochondrial dehydrogenases. Briefly, 1×10^4 cells MeOV PLX-R and MeOV DMSO-R cells were seeded in 96-well plates (Corning) and allowed to adhere overnight. The following day, cells were treated with increasing concentrations (0.01, 0.05, 0.1, 0.5, 1.5, 5, 10 and 20 µM) of PLX4032 or corresponding volume of DMSO, and then cells were left to grow for 72 hrs. Next, 20 µl of Cell Titer Aqueous One Solution were added for one hour in standard conditions (37°C in humidified incubator with 5% CO2). The conversion of tetrazolium to tetrazane takes place only in living cells, and the amount of intracellular formazan can be measured spectrophotometrically. Absorbance was detected at 490 nm using a BioRad iMark microplate reader (BioRad, Milano). Six replicate wells per concentration were used to quantify cell viability.

The increase in resistance, known as fold resistance is calculated through the following equation [131]:

$$Fold\ Resistance = \frac{IC_{50}\ of\ Resistant\ Cell\ Line\ (PLX-R)}{IC_{50}\ of\ Parental\ Cell\ Line\ (DMSO-R)}$$

3.2.2 Clonogenic Assay

Clonogenic assay is an *in vitro* method useful that determines the effectiveness of drug treatment on tumorigenicity, by evaluating the capacity of single cell to produce colonies.

2×10^2 MeOV PLX-R and MeOV DMSO-R cells were seeded in 6-well plates (Corning), and allowed to adhere overnight. Cells were treated with 1.5 µM PLX4032 or with the corresponding dose of DMSO for 24 hrs, then medium was changed and cells were maintained in a drug-free medium for 15 days. Plates were fixed

with ice-cold methanol stained with crystal violet dye solution (0.5% H_2O in 50% Methanol), and colonies consisting of 30 or more cells were counted with an inverted microscope. Images of the colonies were acquired with a digital camera (Huawei P20 PRO).

3.2.3 Wound Healing Assay

Wound healing assay is an *in vitro* method that allow to study quantitatively the directional cell migration in vitro, making a scratch on a cell monolayer and measuring the wound closure by comparison of the images captured at regular intervals.

$3x10^5$ cells were seeded in 12 well plates (Corning), and let them grow. At 95% of confluency, cells were starved with RPMI-1640 supplemented with 0.2% FBS to avoid cell growth. After 24 hr, media was discarded and 1 ml of PBS for each well was added. An artificial wound in the cell monolayer was created using a 200 µl pipette tip and then the monolayer was washed with PBS once. Drug-free medium or 1.5 µM PLX4032 or DMSO medium was added to each well. The migration distance was photographed through an inverted phase microscope (x10) at zero time and after 24 and 48 hr from the treatment. The rate of closure of the wound recovery was determined using Image J software (National Institute of Health, Bethesda, MD, USA).

3.2.4 Intracellular ROS production assay

ROS generation was measured by the use of H2DCFDA (2′-7′-dichlorofluorescin diacetate) assay. H2DCFDA is a non – fluorescent compound, which after diffusion into the cells, is deacetylated by cellular esterases to 2',7'-dichlorofluorescein (H2DCF) that, in presence of ROS, is converted in the oxidized higly-fluorescent molecule DCF which can be detected by

fluorimetric analysis. The generated fluorescence intensity are proportional to the ROS amount.

1×10^4 cells MeOV PLX-R and MeOV DMSO-R cells were seeded in 96-well plates (Corning), and allowed to adhere overnight. The following day, cells were treated 1.5 μM PLX, and incubated for 72 hrs. After treatments, cells were washed with PBS and stained with DCFDA (Thermofisher Scientific) for 30 min at 37°C. Then, cells were incubated with 90% DMSO for 10 min in the dark with shaking [132]. Fluorescence at 485 nm excitation/520 nm emission was measured. Values were normalized to the protein content and expressed as a % of the fluorescence relative to the untreated control.

3.2.5 Metabolic Analysis

8×10^5 cells were seeded in 10 cm dishes and treated for 72 hrs as above described. Cells were tripsinized and counted, and cell culture medium was collected. The media were assayed for measuring the lactate level, while the cells were used for other metabolic evaluations. All the measurements were normalized to cell number.

3.2.5.1 Oxygen Consumption Analysis

Oxygen (O_2) consumption (OCR) was measured by a thermostatically controlled (25°C) oxygraph apparatus equipped with an amperometric electrode (Unisense-Microrespiration, Unisense A/S, Denmark). For this experiment, 2×10^5 cells were permealised with 0.03 mg/ml digitonin for 1 min, centrifuged for 9 min at 1000 rpm and resuspended in an appropriate buffer containing: 137 mM NaCl, 5 mM KCl, 0.7 mM K_2PO_4 and 25 mM Tris HCl pH 7.4. To stimulate complexes I, III and IV pathway, 10 mM pyruvate plus 5 mM malate were added. 20 mM succinate was

_____

added to stimulate the pathway composed by complexes II, III and IV. In order to verify whether OCR is due to electron transport chain, 0.1 mM rotenone or 50 µM antimycin A, specific inhibitors of complex I or complex III, were used to block the first and the second pathway, respectively [133], [134].

3.2.5.2 Evaluation of intracellular ATP and AMP Levels

ATP and AMP levels were measured by the enzyme coupling method, following NAD(P)/NAD(P)H reduction/oxidation at 340 nm. The ATP concentration was measured in a medium containing 100 mM Tris–HCl, pH 7.4, 5 mM $MgCl_2$, 50 mM glucose, 0.2 mM NADP. The assay started after the addition of 4 µg of purified hexokinase and 2 µg of glucose-6-phosphate dehydrogenase.

AMP concentration was measured using a buffer containing 100 mM Tris–HCl, pH 7.4, 5 mM $MgCl_2$, 10 mM phosphoenolpyruvate, 0.15 mM NADH, 0.2 mM ATP. The assay started after the addition of 4 µg of purified kinase plus lactate dehydrogenase and 2 µg of adenylate kinase [135].

3.2.5.3 ATP synthase activity assay

To evaluate ATP synthesis through Fo-F1 ATP synthase, $1x10^5$ cells were incubated in a specific buffer containing 10 mM Tris-HCl pH 7.4, 100 mM KCl, 5 mM KH_2PO_4, 1 mM EGTA, 2.5 mM EDTA, 5 mM $MgCl_2$, 0.6 mM ouabain and 25 mg/ml ampicillin, for 10 min at 37 °C. Afterword, 10 mM pyruvate/5 mM malate or 20 mM succinate were added to induce ATP synthesis through the activation of the complex I, III, IV or the complex II,III,IV pathways, respectively. The reaction was monitored for 2 min, every 30 sec, by the luciferin/luciferase chemiluminescent method and using a GloMax® 20/20n Luminometer (Promega Italia, Milano, Italy). ATP standard solution between 10^{-8} and 10^{-5} M

_____

(luciferin/luciferase ATP bioluminescence assay kit CLSII, Roche, Basel, Switzerland) were used. Data were expressed as nmol ATP produced/min/10^6 cells [133].

In order to evaluate the oxidative phosphorylation efficiency, the P/O ratio was calculated and expressed as the ratio between the concentration of the produced ATP and the amount of consumed oxygen in the presence of respiring substrate and ADP. In physiological conditions, when the oxygen consumption is over, P/O ratio should be around 2.5 and 1.5 after pyruvate/malate or succinate addition, respectively [136].

3.2.5.4 Glucose Consumption Analysis

Glucose consumption was evaluated following the reduction of NADP at 340 nm, through the hexokinase (HK) and glucose-6-phosphate dehydrogenase (G6PD) coupling system. The assay buffer contained 100 mM Tris-HCl, pH 7.4, 2 mM ATP, 10 mM NADP, 2 mM $MgCl_2$, 2 IU of hexokinase, and 2 IU of glucose-6-phosphate dehydrogenase (G6PD). Data were normalized on cell number and expressed as mM glucose consumed/10^6 cells [137].

3.2.5.5 Lactate Release Analysis

Extracellular lactate concentration was measured in the growth medium by spectrophotometry following the reduction of NAD^+ at 340 nm. Samples were suspended in an appropriate buffer containing 100 mM Tris-HCl (pH 8), 5 mM NAD^+ and 1 IU/ml of lactate dehydrogenase. Samples were analysed before and after the addition of 4 μg of purified lactate dehydrogenase [137]. Data were normalized per number of cells and expressed as mM lactate released/10^6 cells.

_____

3.2.6 Protein Extraction and Quantification

After treatment with PLX4032 or DMSO, medium mas removed and then rinsed once with PBS at RT. Then cells were harvested with ice-cold Scraping Buffer pH 7.2 [50 mM Tris-HCl, 150 mM NaCl, 2 mM EDTA, 1 mM EGTA, 1 mM NaF, 1 mM PMSF, 1% Triton and 1% Protease inhibitor Cocktail III], scraped and the lysate was passed through 25-gauge needle, maintained in ice. The lysates were centrifuged at 15000 RPM x at 4°C for 10 min, and then the supernatants were transferred in new tubes and stored at -80°C.

Protein concentration was determined using the Pierce™ BCA protein assay kit (Thermofisher, USA) following manufacturer's instruction.

3.2.7 Western Blotting and Antibodies

Protein aliquots were mixed with 3.5x loading dye [62.5 mM Tris-HCl, pH 6.8, 2% SDS, 25% glycerol, 0.01% bromophenol blue], heated at 95°C for 5 min, separated on 10% or 12% Mini-PROTEAN® TGX™ Precast Gels along with protein marker (Sharpmass VI, Euroclone) and then transferred to PVDF membrane (GE Healthcare, Amersham).

Non-specific binding sites were blocked by incubating membrane in 5% dry non-fat milk in PBS-Tween (80 mM Na_2PO_4, 20 mM NaH_2PO_4, 100 mM NaCl, 0.1% Tween 20) for 1 hr at RT. Then membrane were incubated overnight using rabbit antibody anti p44/42 MAPK (Erk1/2) and anti Phospho-p44/42 MAPK (Cell Signaling Technology Inc., Danvers, MA, USA Upstate, Lake Placid , NY, USA), Phospho-p44/42 MAPK, MITF,GAPDH), anti MITF (Abcam, Cambridgeshire, UK) and GAPDH (Santa Cruz Biotechnology Inc, Santa Cruz, CA, USA) .Membranes were washed 3x in TBS-Tween (20 mM Trizma base, 0.5 M NaCl, 0.1%

_____

Tween 20) and then incubated for 1 hr with the suitable HRP-conjugated secondary antibody (GeHealthcare, Buckingamshire UK). The signal was detected using ECL detection kit (Pierce™ ECL Western Blotting Substrate, ThermoFisher) and analysed with an image densitometer connected to Quantity One Software (Bio-Rad Laboratories, Hercules, CA, USA).

3.2.8 Mitochondrial membrane potential analysis

Mitochondrial membrane potential is evaluated by staining cells with tetrametilrhodamine (TMRM), a fluorescent cell-permeant dye that accumulates in mitochondria proportionally to mitochondrial membrane potential [138]. The fluorescence intensity is quenched when the dye is accumulated within the matrix of mitochondria. 1.5×10^4 DMSO-R and PLX-R cells were seeded on chamber slides (Lab-Tek, Thermo Fisher Scientific Inc, 75 Panorama Creek Drive, Rochester, NY), and let adhere overnight. Cells were treated with 1.5 µM PLX4032 or DMSO for 72 hrs. Then, cells were washed once with PBS and stained with 100 nM TMRM in phenol-red-free RPMI 1640 supplemented with 1% v/v FBS for 40 min at 37°C, 5%CO_2. Forward, the media was replaced for imaging. Images were acquired using an (Leica TCSSP, Nussloch GmbH) microscope and processed using ImageJ software (NIH, USA).

3.2.9 Confocal Microscopy analisys of MITF

1.5×10^4 DMSO-R and PLX-R cells were seeded on chamber slides (Lab-Tek) and let adhere overnight. Cells were treated with 1.5 µM PLX4032 or DMSO for 72 hrs. Then, cells were washed once with PBS and fixed with ice-cold Methanol. Cells were washed again and nonspecific binding sites of the cells were blocked by incubation in 1% BSA in PBS for 1 hr. Then cells were incubated with MITF primary antibody (Abcam). Cells were washed twice

51

PBS and incubated with secondary antibody Alexa Fluor 688 + TOPRO to counterstain nuclei. The glass was fixed with Mowiol. Images were acquired using an (Leica TCSSP, Nussloch GmbH) microscope and processed using ImageJ software (NIH, USA)

3.2.10 Statistical Analysis

Statistical analysis was performed by using GraphPad Prism 6 (San Diego, USA), using one-way ANOVA test with Bonferroni *post hoc* test to determine the statistical significance of observed differences. All data are shown as mean ± standard error mean (SEM) from at least three independent experiments, conducted in triplicates. p values < 0.05 were considered significant.

4 RESULTS

4.1 CHRONIC PLX4032 EXPOSURE INDUCES A PLX4032-RESISTANT PHENOTYPE IN MeOV CELLS

The chronic treatment of BRAF-mutated melanoma with PLX4032 can lead to melanoma progression and resistance to apoptosis. In order to investigate the effects of PLX4032, a BRAF^{V600E}-mutated human metastatic melanoma cell line (MeOV), isolated from a patient, was treated for 6 months with increasing concentrations of PLX4032 (1 nM-1.5 μM) and then maintained in culture with the same drug at the highest concentration. In all experiments, it should be noted that the chronically-PLX4032-treated cells (PLX-R) were compared to the chronically-DMSO-treated ones (DMSO-R).

The identity of melanoma cell lines was verified and certified, comparing MeOV parental cell line profile to the two profiles of resistant cell lines. As shown in Figure 8, the results demonstrated an identical profile of STR sequence loci in all MeOV cell lines, certifying the authenticity of selected cells and demonstrating lack of contamination from other cell lines and microbes.

Cell name	D5S818	D13S317	D7S820	D16S539	VWA	TH01	AM	TPOX	CSF1PO	D21S11	D3S1358	D18S51	Penta E	Penta D	D8S1179	FGA
MeOV NT	12,13	11	7,9	11	15,17	6	x	8	10	33.2	15	12	12	9,12	13	21,22
MeOV DMSOr	12,13	11	7,9	11	15,17	6	x	8	10	33.2	15	12	12	9,12	13	21,22
MeOV PLXr	12,13	11	7,9	11	15,17	6	x	8	10	33.2	15	12	12	9,12	13	21,22

The **MeOV** cell lines show an identical profile.

Figure 8. STR profile of MeOV parental (NT), DMSO-R and PLX-R cell lines. All Me OV cell lines showed an identical STR profile.

To evaluate the state of drug resistance, PLX-R and DMSO-R cells were exposed to increasing concentrations (0.1-20 μM) of PLX4032 for 72 hrs. As shown in Figure 9A, PLX4032 was cytotoxic for DMSO-R cells in a dose-dependent manner (IC50: 0.5 μM) whereas the cytotoxic effect with a 22% reduction of cell viability

_____

was recorded in PLX-R cells at the concentration of 5 µM, reaching IC50 at 18 µM.
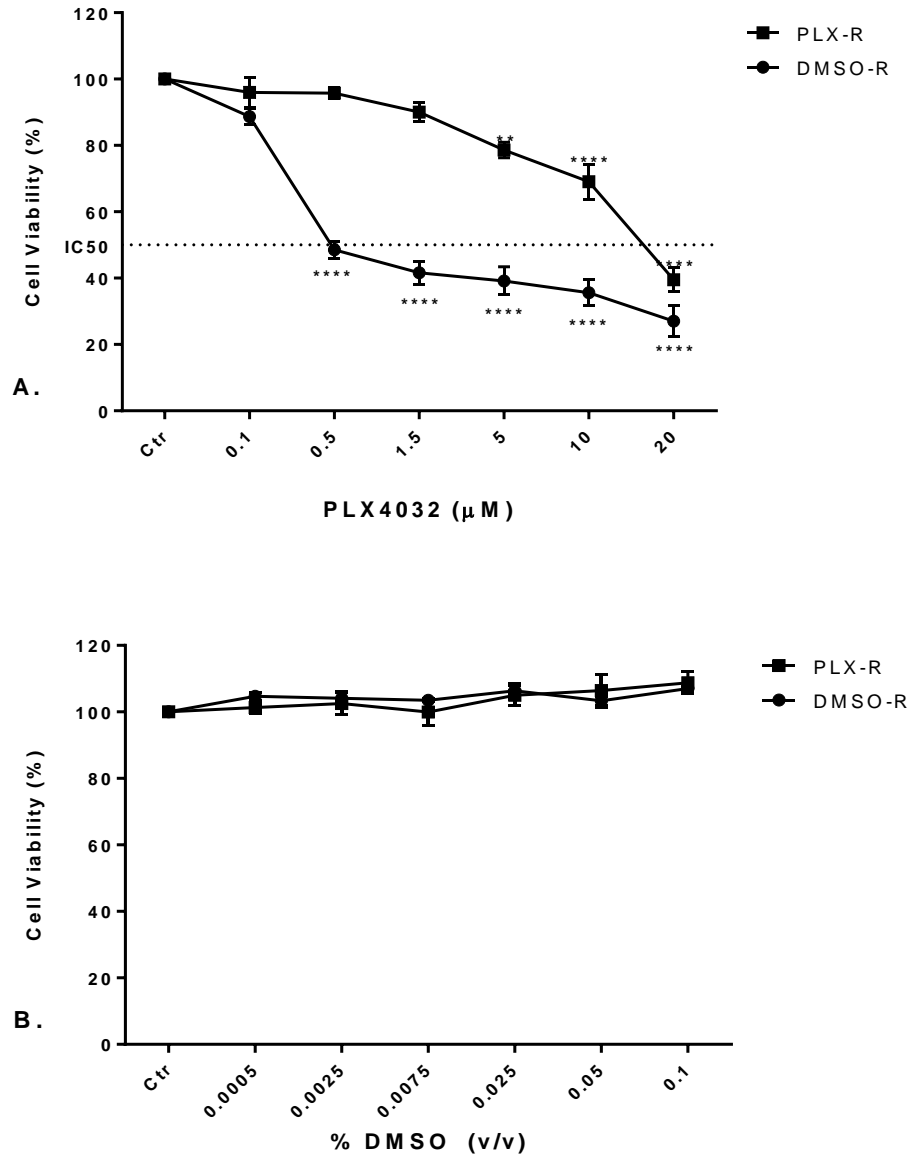

Figure 9. MeOV cells chronically exposed to PLX4032 develop a resistant phenotype. *Cell viability was evaluated by MTS assay in PLX-R and in DMSO-R exposed to increasing concentrations (0.1 µM-1.5 µM) of PLX4032 (A) or DMSO (A) for 72 hrs. The graph summarizes quantitative data of the means ± SEM of four independent experiments. (** p <0.01; **** p < 0.0001 vs. respective Ctr)*

According to equation [131] shown in Materials and Methods, PLX-R showed a 36-fold increased resistance to PLX4032 in comparison with DMSO-R. Notably, the same volume of DMSO utilized to dissolve PLX4032 at all concentrations tested, did not affect *per se* the survival of both cell lines (Fig. 9B).

4.2 THE ACQUISITION OF PLX4032 RESISTANCE IS NOT CONSEQUENTIAL TO THE REACTIVATION OF ERK PATHWAY AND DOES NOT INVOLVE MITF.

Since PLX4032 resistance is classically mediated by MAPK/ERK reactivation [92], the state of ERK activation was investigated. As shown in Figure 10, 24 hr treatment with PLX4032 or DMSO treatment (1.5 µM) did not change ERK protein expression levels in comparison to untreated cells. Instead, the same treatments drastically reduced pERK levels in DMSO-R, demonstrating that PLX4032 was able to exert an inhibitory effect on the V600EBRAF mutation. Unexpectedly, both untreated and acutely-treated PLX-R cells showed low pERK levels (Figure 10), indicating that the acquisition of resistance in this cell line is not effectively due to the classical reactivation of the MAPK/ERK pathway.
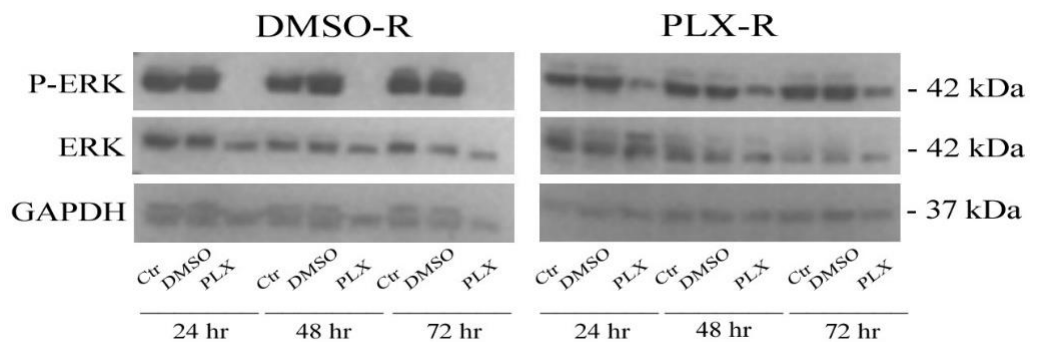

Figure 10. The acquisition of PLX4032 resistance is not dependent on ERK reactivation. *Protein levels of ERK and p-ERK in DMSO-R and PLX-R cells treated for 24,48 and 72 hrs with 1.5 µM PLX4032. Immunoblots shown are representative of three independent experiments. GAPDH is the internal loading control*

_____

However, since MITF is a downstream effector of ERK and it is involved in regulating melanocyte growth and motility [139] its role was investigated. Confocal microscopy shows that in basal conditions both cell populations expressed MITF protein (Figure 11A), and acute treatment with DMSO or PLX did not change MITF protein levels as shown by immunoblot analysis (Figure 11B).
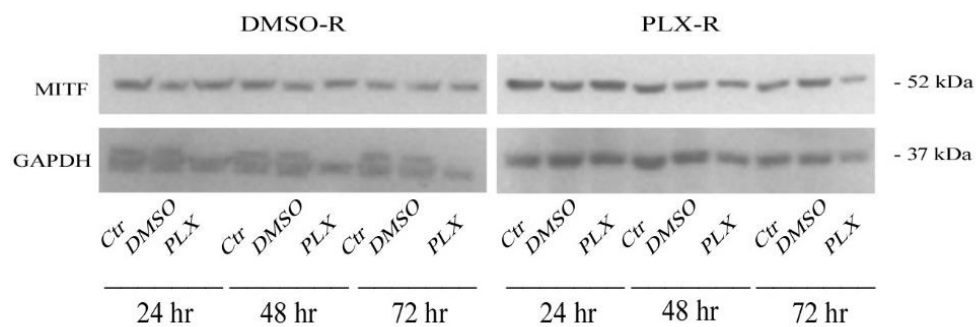
A.
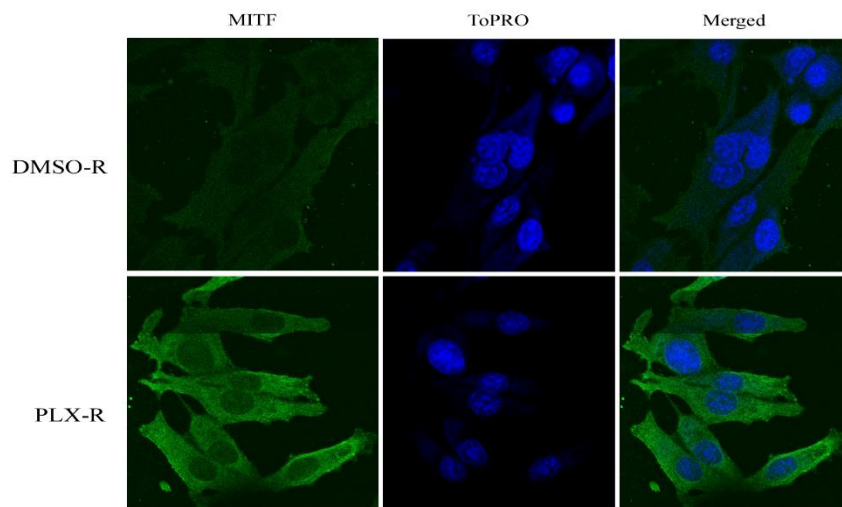
B.

***Figure 11. PLX4032 resistance did not involve MITF expression.** PLx-R and DMSO-R cells were stained with MITF antibody and counterstain with ToPRO.(A.) Protein level of MITF in DMSO-R and PLX-R cells treated for 24,48 and 72 hrs with 1.5 µM PLX4032. Immunoblots shown are representative of three independent experiments. GAPDH is the internal loading control (B.)*

_____

In addition, the clonogenic and the migratory ability of melanoma cells were analyzed. As shown in Figure 12, DMSO-R cells had greater capacity to form colonies in comparison to PLX-R (41 colonies vs. 2.25 respectively). Notably, acute DMSO treatment did not induce changes in the colony formation in either cell line whereas acute PLX exposure enhanced the number of colonies in DMSO-R cells by 90% (75 vs. 41 colonies). The number of colonies of PLX-R cells was not altered by acute treatments with DMSO or PLX.
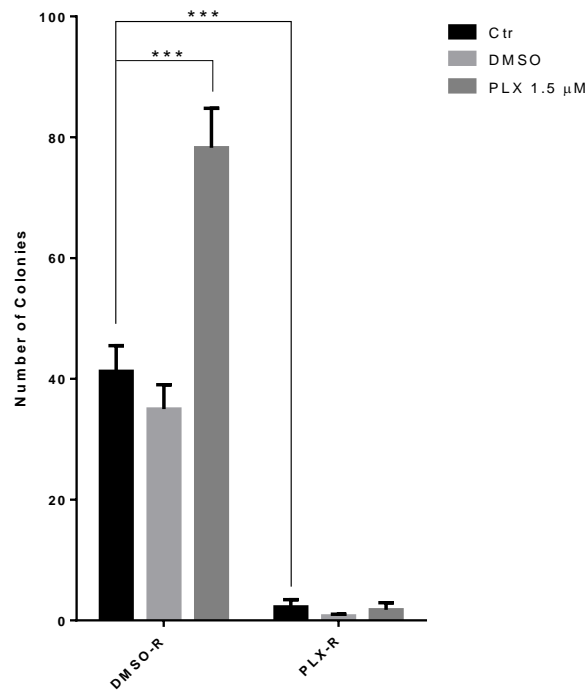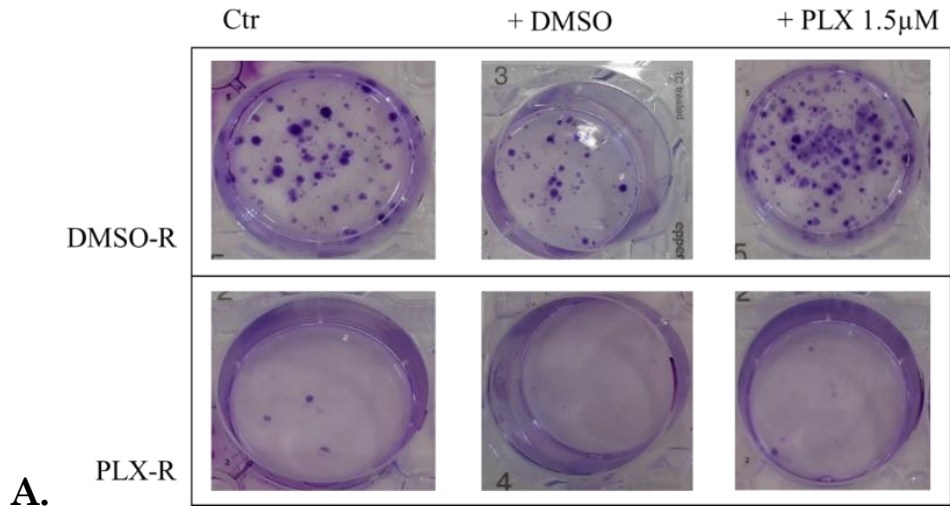
Figure 12. Clonogenic potential of DMSO-R and PLX-R cells. *The ability to form colonies of DMSO-R and PLX-R cells is analyzed by using an anchorage-independent clonogenic assay (**A**). Histogram summarizes quantitative data of means±SEM of three independent experiments (B) (*** p = 0.0001 vs. Control)*

The results obtained by the wound healing assay showed that untreated DMSO-R cells efficiently restored the monolayer after a maximum of 72 hrs, and 24 hr PLX treatment did not modify their migration rate (Figure 13A). On the contrary, the wound-closure

_____

ability of untreated and PLX-treated PLX-R cells was significantly inhibited, suggesting that the acquisition of resistance determines a reduction of cell migratory activity (Figure 13B).

A.
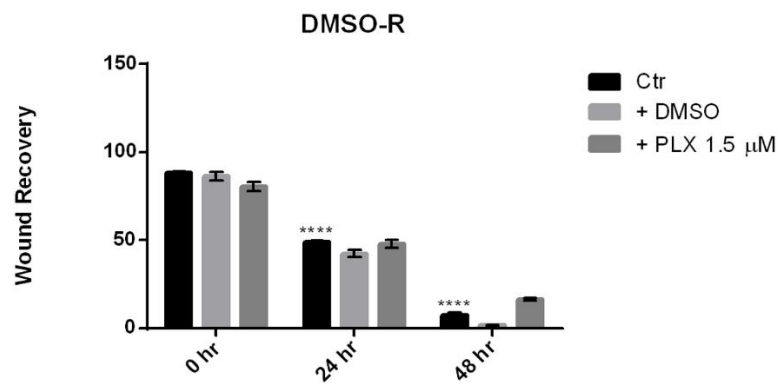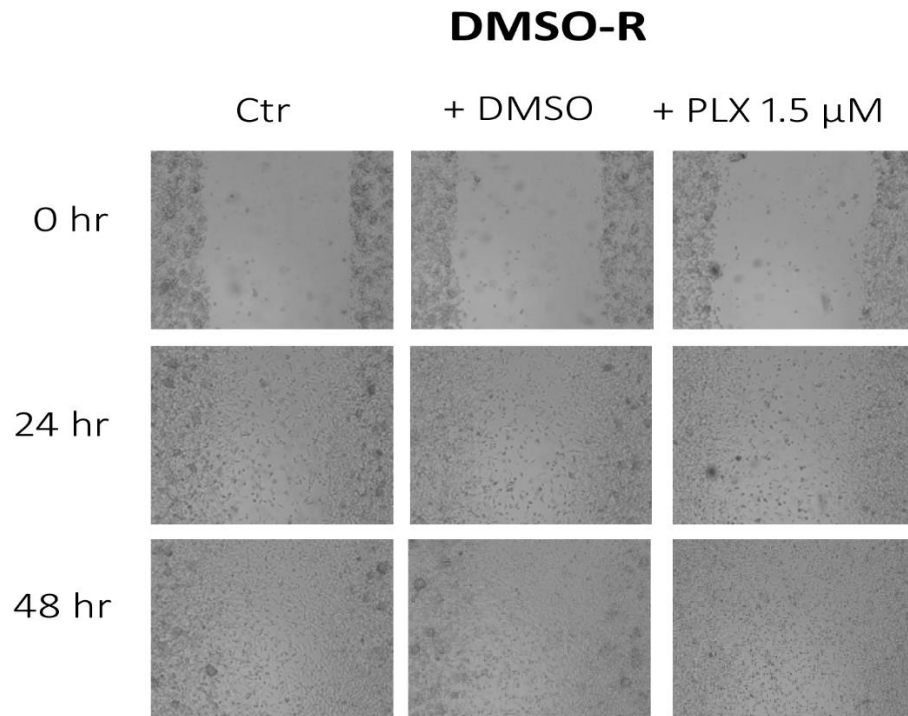
B.

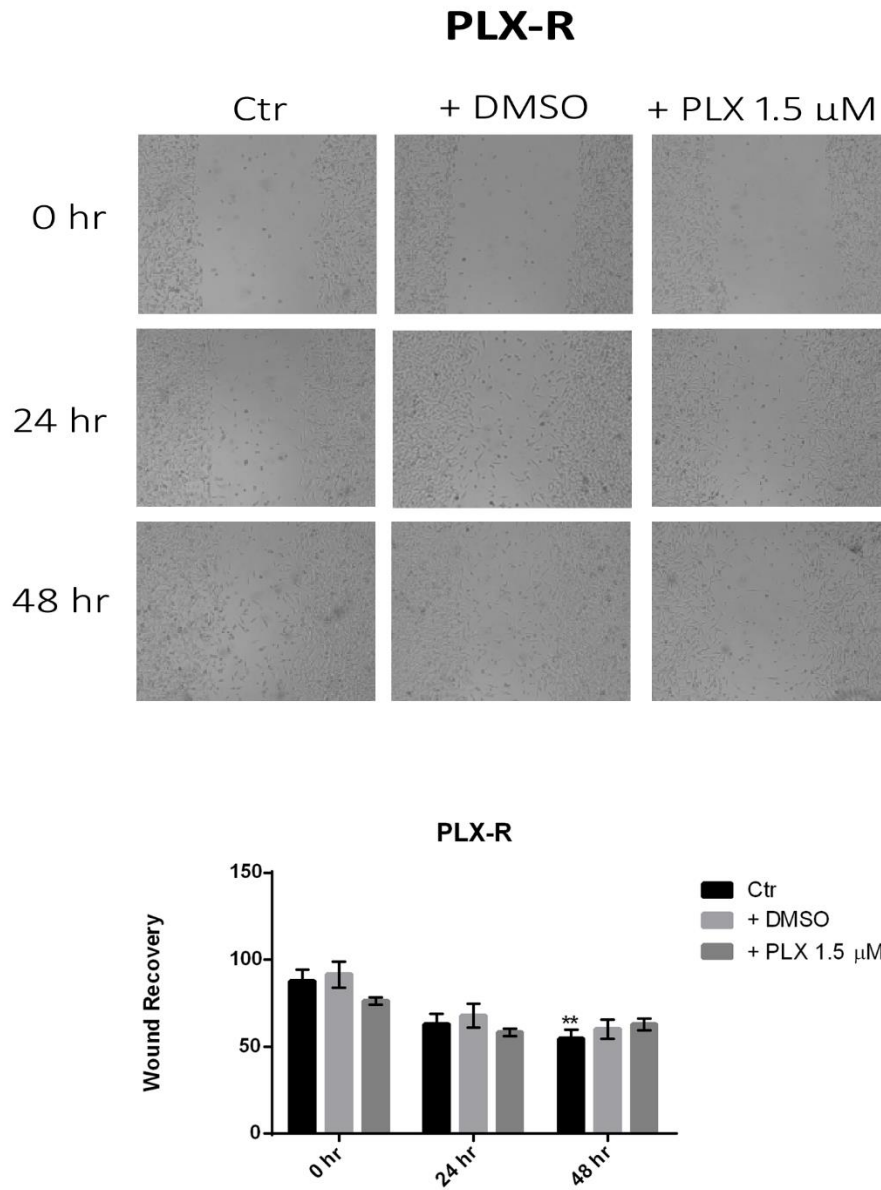*Figure 13. PLX4032 treatment reduces the migratory activity of PLX-R cells. Cell migration of DMSO-R (A) and of PLX-R (B) was evaluated by the scratch assay. The rate of migration was quantified by measuring the distance between the migrating cell boundaries. Histogram summarizes quantitative data of means ± SEM of three independent experiments (** p < 0.01, **** p < 0.0001)*

_____

4.3 THE ACQUISITION OF PLX4032 RESISTANCE CONFERS TO MELANOMA CELLS THE ABILITY TO MAINTAIN AN EFFICIENT OXPHOS METABOLISM

It has been reported that MITF is also involved in cancer metabolic reprogramming [140] since it can control mitochondria biology and, although it is not directly involved in glucose uptake, it stimulates OXPHOS metabolism [140]. As shown in Figure 14, 72 hr PLX4032 exposure did not alter either mitochondria morphology and mitochondria membrane potential of PLX-R cells. In fact, untreated and treated PLX-R cells had elonged mitochondria organized in a functional reticulum whereas DMSO-R cells, after the same treatment, underwent a loss of mitochondria organization and a reduction in mitochondria membrane potential (Figure 14).
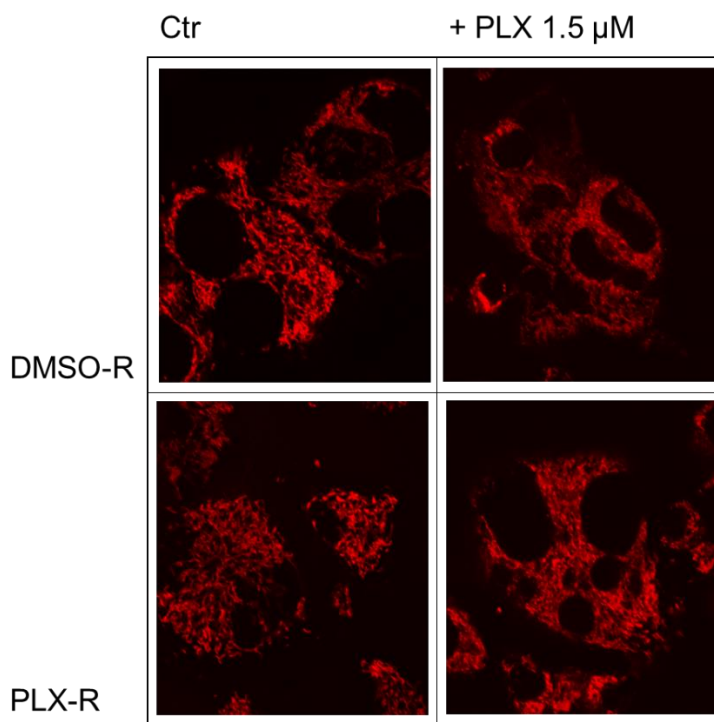

Figure 14. Confocal microscopy analysis of mitochondria morphology and membrane potential in DMSO-R and PLX-R cells. *PLX-R and DMSO-R cells were treated with 1.5 µM PLX4032 for 72 hrs. After treatment, cells were fixed, permeabilized and stained with tetramethilrodamine (TMR). The figures shown are representative of the experiments performed in triplicate.*

_____

However, the changes in mitochondria morphology and potential observed in PLX-treated DMSO-R cells were not accompanied by alterations of ROS production (Figure 15).

A.
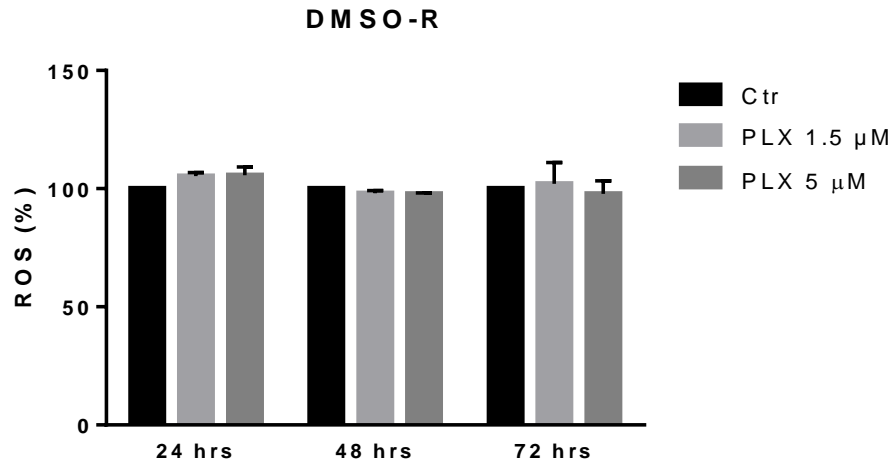
B.

Figure 15. ROS production in DMSO-R and PLX-R cells. ROS production was analyzed in DMSO-R (A) and in PLX-R (B) cells incubated for 24, 48 and 72 hrs with PLX4032 (1.5 or 5 µM). Histograms summarize quantitative data of the means ± S.E.M. of three independent experiments. (**p<0.01 vs. respective Ctr)

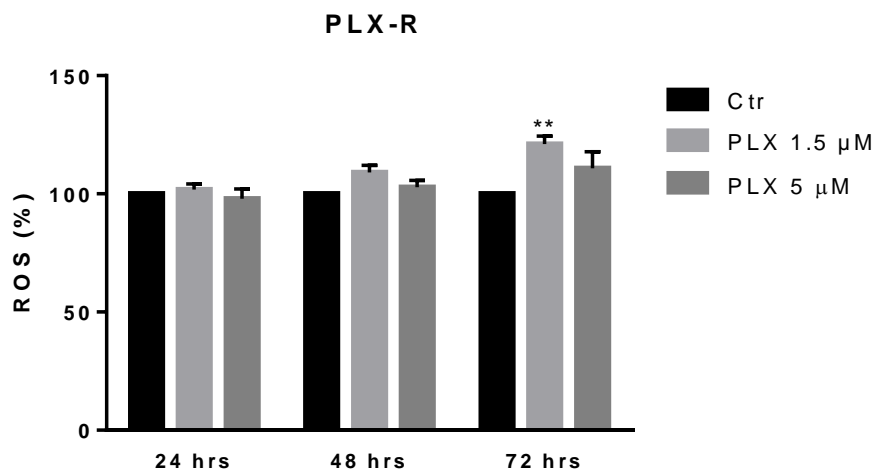Only a 20% increase of ROS production was observed in PLX-R cells after 72 hrs of PLX exposure (Figure 15).

To investigate the role of cell metabolism in the acquisition of drug resistance, the oxygen consumption rate (OCR) and ATP synthesis were analyzed in both cell lines and under all experimental conditions.

In basal conditions, OCR and the ATP synthesis of DMSO-R were 25% higher than the values measured in PLX-R cells (Figure 16 A and B). Moreover, both parameters were not influenced by DMSO treatments in both cell line populations (Figure16 A and B).

Moreover, in DMSO-R cells, PLX4032 exposure reduced OCR and ATP synthesis in a time-dependent manner. In particular, in comparison to untreated cells, the Complex-I linked OCR was reduced by 10%, 21% and 57% after 24, 48 and 72 hrs, respectively and the Complex-II linked OCR decreased by 8%, 16% and 42% respectively. ATP synthesis was reduced by 13%, 30% and 47% in Complex-I after 24, 48 and 72 hrs, respectively and 12%, 35% and 58% in Complex-II respectively (Figure 16 A and B). The same treatments did not induce alterations of OCR and ATP synthesis in PLX-R cells (Figure16 A and B).

A.
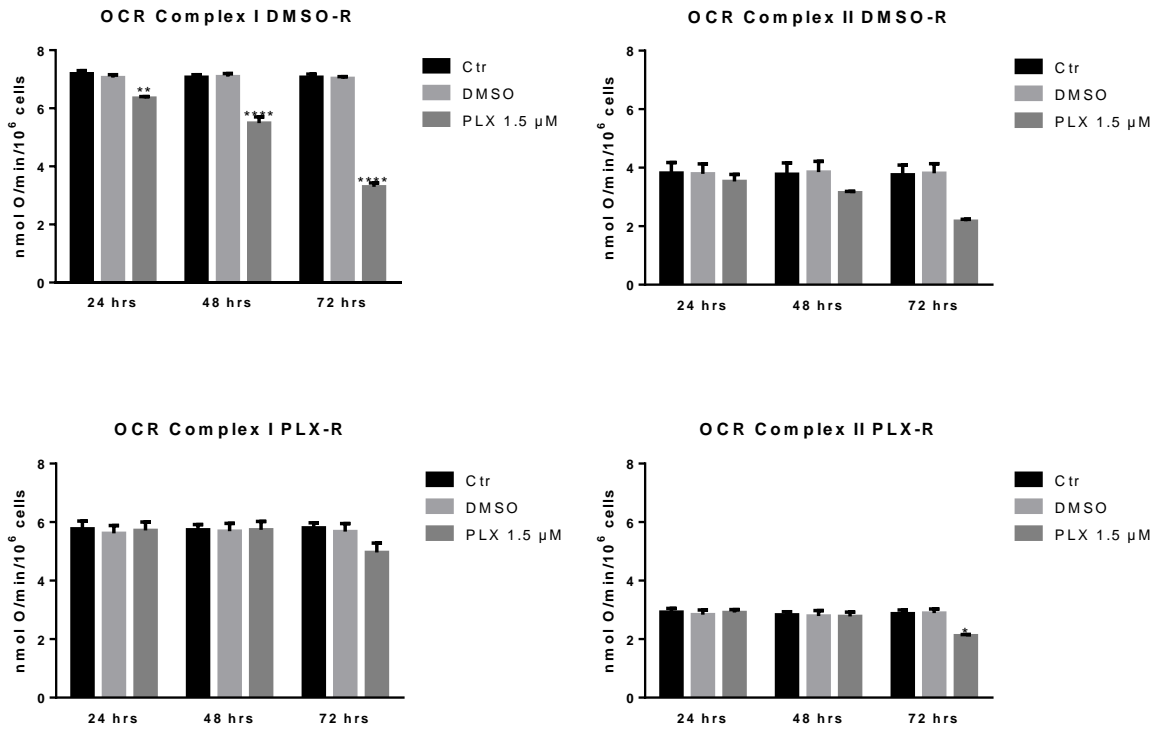
B.
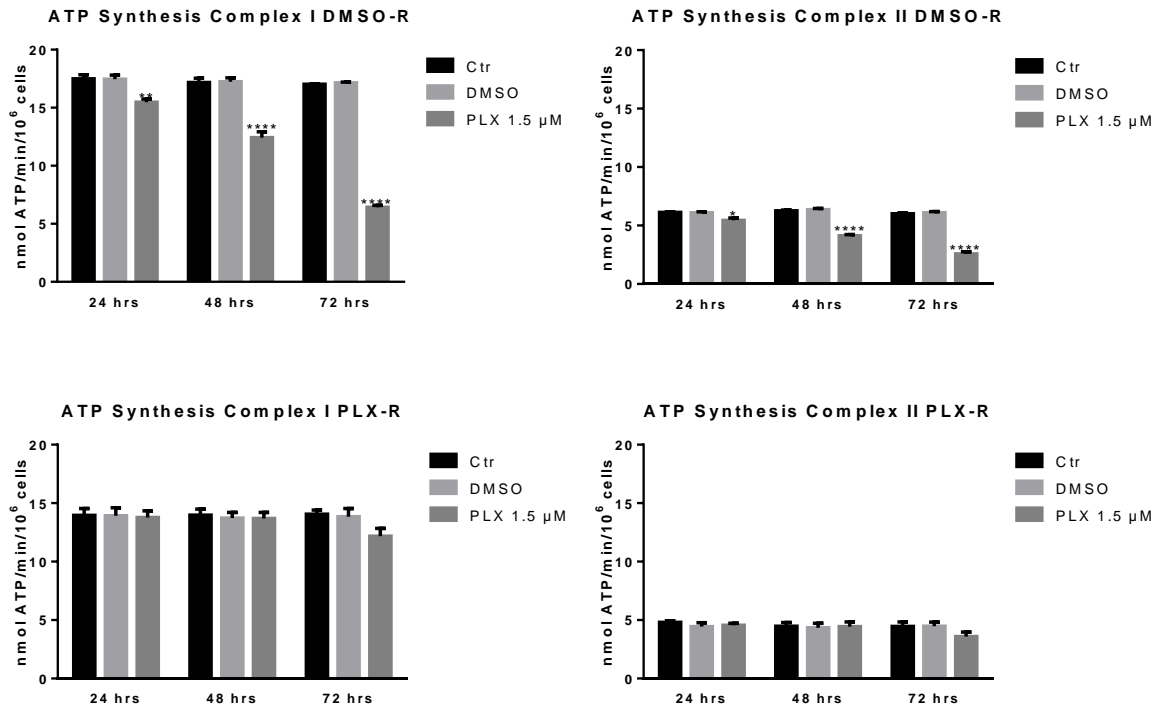
Figure 16.Evaluation of oxygen consumption rate and ATP synthesis in DMSO-R and PLX-R cells. The ability of cells to consume oxygen and to produce ATP by OXPHOS was evaluated using complex I-linked substrates (pyruvate, malate) and complex II-linked substrate (succinate), that are physiological substrates stimulating the mitochondrial OXPHOS. The oxygen consumption rate (OCR) (A) was evaluated in untreated and in 1.5 μM PLX4032-treated (24, 48 and 72 hrs) DMSO-R and PLX-R cells. Results were reported as nmol $O_2/min/10^6$ cells. B. ATP synthesis was measured in untreated and in 1.5 μM PLX4032-treated (24, 48 and 72 hrs) DMSO-R and PLX-R cells. Results were reported as nmol $ATP/min/10^6$ cells.
Histograms summarize quantitative data of means ± S.E.M. of three independent experiments (*p< 0.05 vs. respective Ctr ; **p< 0.01 vs. respective Ctr; ****p< 0.0001 vs. respective Ctr).

Moreover, in order to evaluate the oxidative phosphorylation efficiency, the P/O ratio was calculated and expressed as the ratio between the concentration of the produced ATP and the amount of consumed oxygen in the presence of respiring substrates and ADP. Under physiological conditions, when the oxygen consumption is over, P/O ratio should be around 2.5 and 1.5 after pyruvate/malate or succinate addition, respectively [141].

_____

As shown in Table1, in untreated and DMSO-treated DMSO-R cells, the P/O ratio was comparable to the physiological level (2.5 for Complex I and 1.5 for Complex II) reported by Hinkle [141]. In addition, after 72 hr PLX4032 exposure, the P/O ratio was reduced by 21.6%, suggesting a partial OXPHOS uncoupling. In PLX-R cells all treatments did not induce alterations of P/O ratio which was always maintained at the physiological levels (Table 1).

DMSO-R P/O Ratio

	24 hrs		48 hrs		72 hrs	
	Complex I	Complex II	Complex I	Complex II	Complex I	Complex II
Ctr	2.43±0.03	1.45±0.04	2.43±0.06	1.47±0.08	2.41±0.06	1.45±0.04
DMSO	2.47±0.03	1.46±0.05	2.43±0.05	1.50±0.07	2.44±0.02	1.46±0.01
PLX 1.5 µM	2.44±0.10	1.55±0.21	**2.26±0.01***	**1.35±0.04***	**1.96±0.21***	**1.16±0.13***

PLX-R P/O Ratio

	24 hrs		48 hrs		72 hrs	
	Complex I	Complex II	Complex I	Complex II	Complex I	Complex II
Ctr	2.42±0.06	1.65±0.09	2.44±0.09	1.58±0.10	2.42±0.05	1.55±0.14
DMSO	2.48±0.14	1.57±0.14	2.41±0.05	1.55±0.12	2.44±0.09	1.55±0.15
PLX 1.5 µM	2.41±0.11	1.57±0.14	2.39±0.08	1.60±0.14	2.46±0.06	1.70±0.32

Table 1. PLX-R cells maintain an efficient OXPHOS after acute PLX4032 exposure. P/O ratio values after PLX4032 and DMSO treatments of DMSO-R and PLX-R cells, calculated and expressed as the ratio between the concentration of the produced ATP and the amount of consumed oxygen in the presence of respiring substrates and ADP (*p<0.05 vs. respective Ctr)

In addition, as shown in Figure 17, untreated DMSO-R and PLX-R cells had comparable intracellular ATP and AMP levels, at all three considered timepoints (24, 48 and 72 hrs) and DMSO exposure did not influence these parameters. In conformity with the results above reported, PLX4032 treatment affected in a time-dependent manner ATP and AMP levels of DMSO-R cells. In fact,

_____

ATP levels were reduced by 10%, 21% and 57% after 24, 48 or 72 hrs respectively, in comparison to untreated DMSO-R cells (Figure 17 A), while AMP levels increased by 13%, 30% and 47% (Fig. 16, C). In PLX-R cells all treatments did not induce changes in ATP levels (Figure 17 B) and only 72 hr-exposure to PLX4032 was able to increase the intracellular levels of AMP by 14% in comparison to untreated cells (Figure 17 D). Accordingly with these findings, the ATP/AMP ratio was reduced by 33%, 40% and 70% in 24, 48 and 72 hr PLX-treated DMSO-R cells (Figure 17 E) whereas it was not modified in PLX-R until 48 hrs of PLX treatment with a 10% reduction after 72 hrs (Figure 17 F).

_____
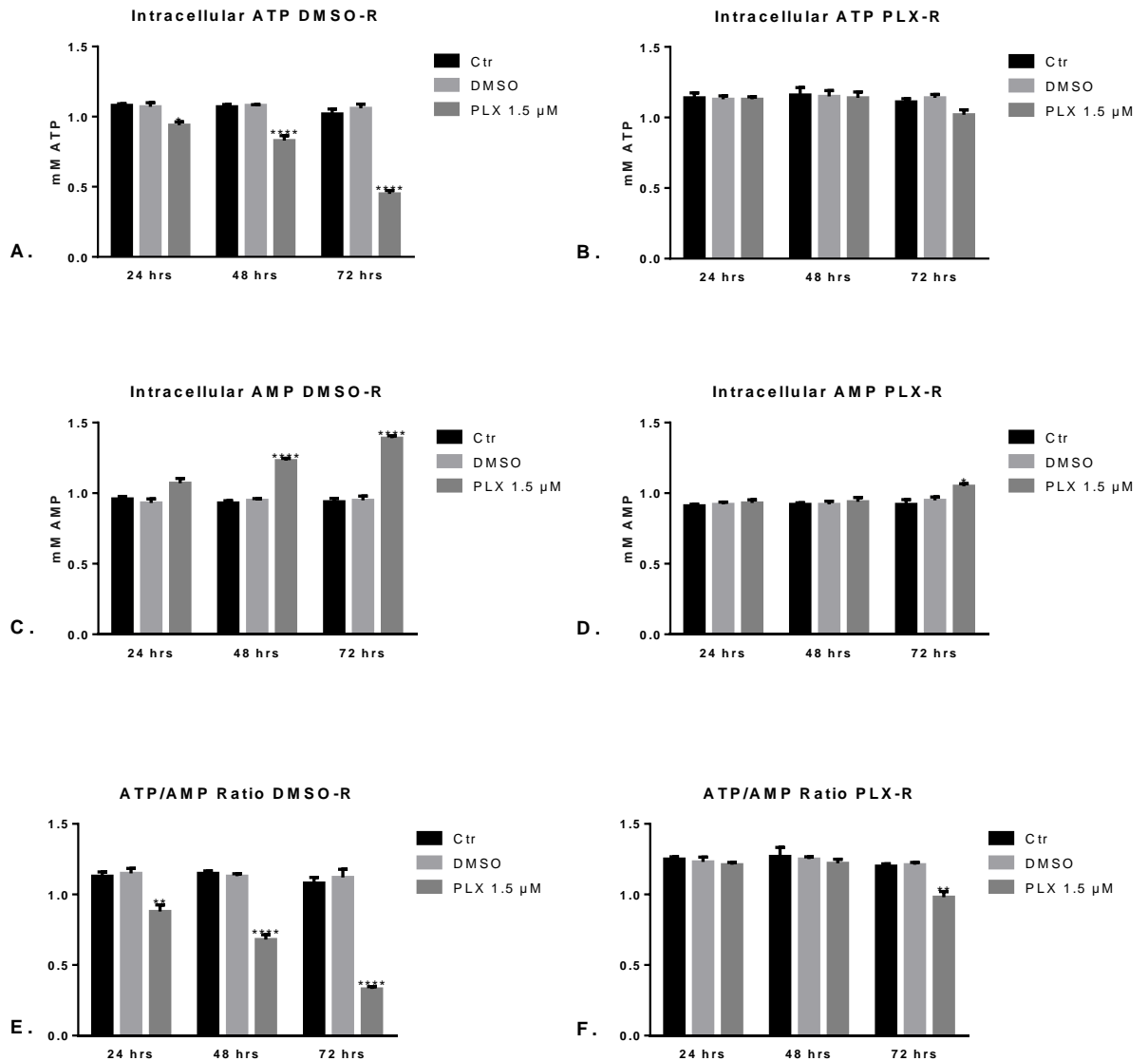
Figure 17. PLX-R cells maintain the energetic status after PLX exposure. ATP (A,B), AMP (C,D) and ATP/AMP ratio (E,F) were evaluated in untreated and in PLX-treated DMSO-R (A) and PLX-R cells. Histograms summarize quantitative data of means ± S.E.M. of three independent experiments (*p<0.05 vs. respective Ctr ; **p<0.01 vs. respective Ctr; ****p<0.0001 vs. respective Ctr)

In order to better characterize the metabolic profile of PLX resistant cells, the rate of glucose consumption, lactate formation, as well as the activity of lactate dehydrogenase (LDH) was evaluated. As shown in Figure 18, DMSO treatment did not induce changes in glucose consumption (Figure 18 A and B) and in lactate

_____

release (Figure 18 C and D) in both cell populations. Analogously, PLX4032 exposure did not affect the glucose consumption (Figure 18 B) and the lactate release (Figure 18 D) of PLX-R cells while, in DMSO-R cells, it increased significantly both parameters in a time-dependent manner, in comparison to respective control (Figure 18 A and C). In addition, as shown in the panels C and D of Figure 18, untreated DMSO-R cells were more able to release lactate (+58%) than PLX-R cells. In regards to the analysis of LDH activity, DMSO treatment did not induce changes in both cell lines. PLX4032 exposure did not affect LDH activity in PLX-R cells (Figure 18 E and F) while, according to the results of lactate release, it caused a time-dependent increase in LDH activity in DMSO-R cells (Figure 18 E).
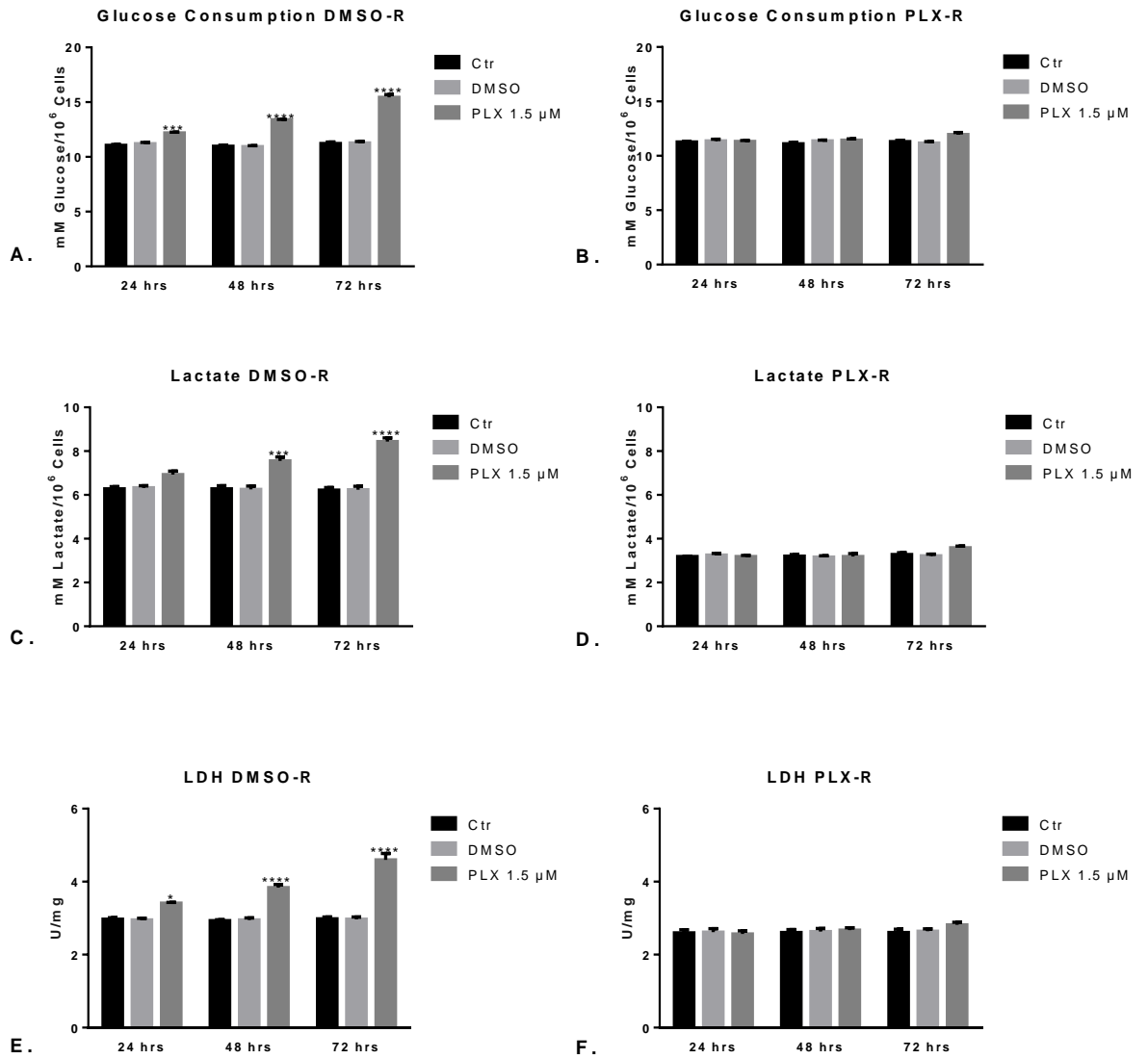
Figure 18. Analysis of glucose consumption, lactate release and LDH activity in DMSO-R and PLX-R cells. *PLX exposure did not induce metabolic switch in PLX-R cells. Upper panels: Glucose consumption was evaluated in untreated and in DMSO or PLX-treated (24, 48 and 72 hrs) DMSO-R (**A**) and PLX-R cells (**B**). Values are expressed as mM glucose/10⁶ cells. Intermediate panels: Extracellular lactate concentration was evaluated in untreated and in DMSO or PLX-treated (24, 48 and 72 hrs) DMSO-R (**C**) and PLX-R cells (**D**). Values are expressed as mM lactate/10⁶ cells. Lower panels: Lactate dehydrogenase (LDH) activity was evaluated in untreated and DMSO or PLX-treated (24, 48 and 72 hrs) DMSO-R (**E**) and PLX-R cells (**F**). Results are reported as U/mg (lactate µmol/min/mg of total protein). Histograms summarize quantitative data of means ± S.E.M. of three independent experiments (***p<0.001 vs. respective Ctr; ****p< 0.0001 vs. respective Ctr).*

5 DISCUSSION

Melanoma is one of the most lethal forms of skin cancer and its incidence continues to increase worldwide [142].

A common abnormality found in up to 60% of melanomas and their metastases is an activating mutation in the proto-oncogene BRAF, which substitutes codon 600 from valine to glutamic acid (V600E) and results in a constitutively activated BRAF oncogene and the activation of MEK1/2 and, ultimately, of the downstream MAPK target, ERK [143]. The activated BRAF→MEK→ERK pathway, resulting from the BRAF^{V600E}, has been shown to drive melanoma cell proliferation and is implicated in the poor therapeutic outcome.

The relationship between the activated ERK pathway, the increased melanoma cell growth and the BRAF^{V600} mutation has led to target this pathway in the treatment of melanoma. In this context, PLX4032/Vemurafenib, has been found to induce tumor regression in a high percentage of patients with BRAF^{V600E}-positive metastatic melanoma [74]. However, although treatment with this selective inhibitor can control tumor growth, it rarely leads to tumor eradication due to an acquired drug resistance [86]. The development of the acquired resistance is usually associated with the reactivation of the MAPK signalling pathway through NRAS or KRAS mutations [91] or alternatively, in the reactivation of parallel pathways such as PI3K/AKT [92], or enhanced activity of Tirosine-Kinase Receptor (RTK) [93], [99]. In view of these limitations, new protocols have been designed in which BRAF-targeted therapies have been associated with MEK inhibitors (MEK-i), such as Trametinib or Cobimetinib [144].

However, MEK-i have been unsuccessful both in preclinical models and in patients with resistance to BRAF-inhibitors (BRAF-

_____

i) suggesting that other compensatory pathways would be involved.

Thus, these observations highlight urgent need to increase the knowledge of the mechanisms underlying therapy resistance in melanoma in order to find new therapeutic strategies to overcome resistance to BRAF-i. In this context, it is important not limiting the research on the study of molecular pathways, but extending focus also on the involvement of metabolism in the acquired resistance.

Given that tumors are heterogeneous [131], the pre-clinical model, which is used to study *in vitro* the mechanisms of resistance, needs to predict the heterogeneous response of cancer cells *in vivo* [131]. Therefore, the first aim of this PhD thesis was to find an *in vitro* model of a BRAF^{V600E}-mutated human melanoma cell line, in order to obtain a more realistic model of drug resistance in comparison with the commonly used stabilized cancer cells.

The model of PLX4032 resistance used in this study is innovative since it is performed by treating human melanoma cells, isolated from patient's biopsies, with increasing concentrations of PLX32 for a long-term period (6 months). In our model, melanoma cells adapt to grow in the presence of the drug, while the drug is slowly increased. The rate fold increased resistance together with the method of selection places this new model in the category of "High-level laboratory model" as defined by Mc Dermott [131]. This type of model is classified as "stably resistant", and the molecular changes associated with the mechanisms of resistance are easily identifiable and analysable. In addition, our selection adds the pulsed procedure, which provides a recovery time for the cells, typical of "Clinical relevant model".

This procedure together with the exposure to increasing drug concentrations starting from a low dosage (typical of ""High-level

laboratory model"), tries to mimic the conditions of cancer patients during the therapy [131].

In the scientific literature, *in vitro* models, that are employed for studying chemoresistance in melanoma, lead to a selection of melanoma cells, isolated from human specimens, by using high concentrations of PLX administered for a shorter period of exposure (5 days) [131], [145] or from stabilized melanoma cell lines treated with PLX for different times (2-3 weeks up to 2-3 months) [99].

Therefore, our model can better mimic the *in vivo* condition and the characterization of PLX4032-sensitive and -resistant BRAF^{V600E} mutant melanoma cell lines may provide more promising information about the molecular mechanisms that dictate sensitivity and resistance to PLX4032.

Among the key factors potentially responsible for the reactivation of pro-survival signaling pathways, leading to an acquired resistance to BRAF-i therapy, melanoma cell metabolism has been demonstrated to play a relevant role [146].

In this context, it is widely observed that the metabolic profile of cancer is very heterogeneous because metabolic pathways are intrinsically driven by oncogenic mutations, tumor suppressor gene inactivation and aberrant activation of proliferative pathways [147]. Metastatic melanoma are characterized by their strict dependence on glucose or glutamine for proliferation [117] and in approximately 90% of melanomas the metabolic phenotype is associated with low mitochondrial bioenergetic activity [50].

In this study, it has been demonstrated that chronic PLX exposure of human melanoma cells leads to the suppression of glycolysis, the maintenance of a functional mitochondrial reticulum and the reactivation of OXPHOS as a mechanism of metabolic adaptation that limits the efficacy of BRAF inhibitors. On the other hand,

PLX-sensitive melanoma cells have a glycolytic profile, accompanied by a lower ATP synthesis and a loss of mitochondria organization.

This metabolic reprogramming is commonly found in cancer [148] and is recently considered as an hallmark of cancer [149] but its role in drug resistance needs to be further investigated.

Moreover, changes in the metabolic profile of cancer cells are accompanied by phenotypic changes that may be related to each other.

In fact, in our model, DMSO-resistant cells, differently from the resistant counterpart, show an evident glycolytic flux and have a better capacity to migrate.

According to these results, Keren Yizhak et al. by using a computational model-based investigation across cancer cell lines, showed that the ratio between glycolytic pathway and oxidative ATP flux rate is significantly associated with cancer migratory behaviour [150]. Moreover, the correlation between glycolytic activity and migration was confirmed also by De Bock *et al* showing that endothelial cells silenced for the glycolytic regulator PFKB3 have an impaired cell migration capacity.

However, the metabolic machinery of melanoma cells is not rigid and mitochondria are likely to have a key role in the metabolic flexibility of melanoma.

Recently, it has been demonstrated that metastatic melanomas with activation of the oncogenic BRAF/MAPK pathway have suppressed levels of microphthalmia-associated transcription factor (MITF) [151], which is the melanocyte lineage factor and, consequently the depletion of its target PGC1α, the transcription factor responsible for mitochondrial biogenesis [152] leading to a decreased oxidative metabolism.

_____

In our cellular model, MITF is expressed and equally present in PLX-sensitive and PLX-resistant melanoma cells. Moreover, the production of reactive oxygen species (ROS) is lightly enhanced in PLX-R cells after 72 hrs of PLX exposure.

Therefore, an efficient mitochondrial activity and the ability to maintain low levels of ROS might contribute to sustain PLX resistance favoring melanoma cell survival.

Recently, Piskounova et al. found that melanoma cells, isolated from the circulation and from metastatic sites, displayed higher levels of ROS than those from the primary tumor, and that the metastatic tumors showed a reversible elevation in the production of NAPDH, which has been correlated with an increased regeneration of glutathione (GSH) [153]. Since GSH is essential to guarantee a limited production of ROS and its homeostasis is crucial in cancer cell survival [154], further studies are needed to better investigate the oxidative metabolism of PLX sensitive and PLX resistant cells in order to identify the Achille's heel of PLX resistant melanoma cells.

Then, the long-term treatment of BRAF-mutated melanoma with PLX4032, which reduces the capacity of melanoma cells to form colonies and to migrate, induces oxidative phosphorylation that might represent an adaptive metabolic program which is able to limit the efficacy of the therapy.

6 CONCLUSION

In contrast to cytostatic shotgun chemotherapy, new cancer drugs are "targeted" and directed towards molecular factors controlling cancer expansion processes. To date, the use of these biological compounds unfortunately leads as other therapy to the selection of small resistant sub-populations of tumor cells after a prolonged treatment with the drug.

However, given the variability of the mechanisms involved, overcoming the resistance to BRAF inhibitors remains challenging and there is an ongoing effort to identify biomarkers related to the molecular and metabolic features of the tumor which may determine the efficacy of targeted therapies.

7 PUBLICATIONS

SCIENTIFIC REP🞧RTS

Etoposide-resistance in a neuroblastoma model cell line is associated with 13q14.3 mono-allelic deletion and miRNA-15a/16-1 down-regulation

Barbara Marengo[1], Paola Monti[2], Mariangela Miele[2], Paola Menichini[2], Laura Ottaggio[2], Giorgia Foggetti[2,3], Alessandra Pulliero[4], Alberto Izzotti[2,4], Andrea Speciale[1], Ombretta Garbarino[1], Nicola Traverso[1], Gilberto Fronza[2] & Cinzia Domenicotti[1]

Drug resistance is the major obstacle in successfully treating high-risk neuroblastoma. The aim of this study was to investigate the basis of etoposide-resistance in neuroblastoma. To this end, a MYCN-amplified neuroblastoma cell line (HTLA-230) was treated with increasing etoposide concentrations and an etoposide-resistant cell line (HTLA-ER) was obtained. HTLA-ER cells, following etoposide exposure, evaded apoptosis by altering Bax/Bcl2 ratio. While both cell populations shared a homozygous *TP53* mutation encoding a partially-functioning protein, a mono-allelic deletion of 13q14.3 locus, where the P53 inducible miRNAs 15a/16-1 are located, and the consequent miRNA down-regulation were detected only in HTLA-ER cells. This event correlated with BMI-1 oncoprotein up-regulation which caused a decrease in p16 tumor suppressor content and a metabolic adaptation of HTLA-ER cells. These results, taken collectively, highlight the role of miRNAs 15a/16-1 as markers of chemoresistance.

Neuroblastoma (NB) is one of the most common extra-cranial solid tumors in childhood and it is characterized by high clinical and biological heterogeneity[1,2]. Among the genetic changes most frequently associated with the aggressive cancer phenotype, the amplification of the MYCN proto-oncogene is an important predictor of high-risk NB[3]. Although most high-risk NB patients initially respond to therapy, a majority of these patients will relapse with treatment-resistant disease. It has been found that approximately 50% of relapsed NBs are associated with the inactivation of the *TP53* tumor-suppressor gene pathways[4].

The loss of function of the P53 protein may derive either from the mutations of the *TP53* gene[5], the interaction of P53 with its endogenous inhibitor MDM2[6], or from the transcriptional and/or post-transcriptional regulation of P53 and P53-dependent genes[7].

In NB, *TP53* mutations are rare at diagnosis[8] but P53 inactivation occurs relatively often (~50%) following therapeutic treatment[9]. However, the molecular mechanisms leading to P53 impairment in treatment-resistant diseases have not yet been elucidated. In this context, we have recently demonstrated that HTLA-230, a MYCN-amplified human NB cell line chronically treated with the clinically-used drug etoposide[10], developed etoposide-resistance and also acquired a multi-drug resistance (MDR) phenotype, thus becoming able to efficiently repair DNA damage and evade apoptosis[11]. Since apoptotic failure, a critical hallmark of cancer[12], is often determined by the loss of the tumor suppressor activity of P53, herein we initiated the investigation of the role of the P53 pathway in the acquisition of the MDR phenotype.

[1]Department of Experimental Medicine, General Pathology Section, University of Genova, Genova, Italy. [2]UOC Mutagenesis and Oncologic Prevention, IRCCS Ospedale Policlinico San Martino, Genova, Italy. [3]Yale Cancer Center, Yale University School of Medicine, New Haven, Connecticut, USA. [4]Department of Health Sciences, University of Genova, Genova, Italy. Barbara Marengo, Paola Monti, Gilberto Fronza and Cinzia Domenicotti contributed equally. Correspondence and requests for materials should be addressed to C.D. (email: Cinzia.Domenicotti@unige.it)

Review Article

MYC Expression and Metabolic Redox Changes in Cancer Cells: A Synergy Able to Induce Chemoresistance

Barbara Marengo [iD],[1] **Ombretta Garbarino** [iD],[1] **Andrea Speciale**,[2] **Lorenzo Monteleone**,[1] **Nicola Traverso** [iD],[1] **and Cinzia Domenicotti** [iD][1]

[1]*Department of Experimental Medicine, General Pathology Section, University of Genova, Italy*
[2]*UOC Mutagenesis and Oncologic Prevention, Ospedale Policlinico San Martino, Genova, Italy*

Correspondence should be addressed to Barbara Marengo; barbara.marengo@unige.it

Chemoresistance is due to multiple factors including the induction of a metabolic adaptation of tumor cells. In fact, in these cells, stress conditions induced by therapies stimulate a metabolic reprogramming which involves the strengthening of various pathways such as glycolysis, glutaminolysis and the pentose phosphate pathway. This metabolic reprogramming is the result of a complex network of mechanisms that, through the activation of oncogenes (i.e., MYC, HIF1, and PI3K) or the downregulation of tumor suppressors (i.e., TP53), induces an increased expression of glucose and/or glutamine transporters and of glycolytic enzymes. Therefore, in order to overcome chemoresistance, it is necessary to develop combined therapies which are able to selectively and simultaneously act on the multiple molecular targets responsible for this adaptation. This review is focused on highlighting the role of MYC in modulating the epigenetic redox changes which are crucial in the acquisition of therapy resistance.

1. Cancer Metabolic Reprogramming

Metabolic reprogramming is an early event in the carcinogenic process, and it is involved in the development of malignancy and the acquisition of most cancer hallmarks [1]. The first metabolic phenotype observed in cancer cells was described by Otto Warburg, a German biochemist, as a shift from oxidative phosphorylation (OXPHOS) to aerobic glycolysis to generate lactate and ATP even in the presence of O_2 (i.e., Warburg effect) [2]. Since the Warburg effect is also found in tumor cells with intact and functional mitochondria, it is reasonable to assume that it could represent a strategy adopted by cancer cells, not only to cope with the greater energy demands but also to reduce oxidative stress, preserving cells from oxidative death [3]. In this regard, reactive oxygen species (ROS), maintained at "physiological" levels, have been demonstrated to activate redox signaling pathways involved in cell proliferation and survival [4, 5].

Over the past decade, numerous studies have supported the hypothesis that the Warburg effect can be explained by the alterations in multiple signaling pathways resulting from mutations of oncogenes and tumor suppressor genes [6, 7]. Indeed, tumor metabolic reprogramming involves the activation of key metabolic pathways such as glycolysis, the pentose phosphate pathway, and glutaminolysis [8].

In this regard, it has been demonstrated that the glycolytic metabolic switch is due to a marked slowing down of the conversion of phosphoenolpyruvate into pyruvate, a reaction catalyzed by pyruvate kinase (PKM) [9]. Furthermore, in cancer cells, it has been observed that the presence of the low-activity dimeric form of PKM2 promotes the conversion of pyruvate to lactate [10] and that the increased levels of lactic acid detected in cancer patients are related to rapid tumor growth and high levels of metastases [11]. Moreover, considering that most chemotherapeutic agents are weak bases, the presence of lactic acid, generating acidity, induces the ionization of the drugs which, in their modified

8 BIBLIOGRAPHY

[1] E. R. Cantwell-Dorris, J. J. O'Leary, and O. M. Sheils, "BRAFV600E: Implications for carcinogenesis and molecular therapy," *Molecular Cancer Therapeutics*. 2011.

[2] M. Brenner and V. J. Hearing, "The protective role of melanin against UV damage in human skin," *Photochemistry and Photobiology*. 2008.

[3] L. Garibyan and D. E. Fisher, "How sunlight causes melanoma," *Current Oncology Reports*. 2010.

[4] I. T. Valyi-Nagy, G. Hirka, P. J. Jensen, I. M. Shih, I. Juhasz, and M. Herlyn, "Undifferentiated keratinocytes control growth, morphology, and antigen expression of normal melanocytes through cell-cell contact," *Lab. Investig.*, 1993.

[5] G. A. Scott and A. R. Haake, "Keratinocytes regulate melanocyte number in human fetal and neonatal skin equivalents," *J. Invest. Dermatol.*, 1991.

[6] J. E. Gershenwald *et al.*, "Melanoma staging: Evidence-based changes in the American Joint Committee on Cancer eighth edition cancer staging manual," *CA. Cancer J. Clin.*, 2017.

[7] A. Chafidz, M. Kaavessina, S. Al-Zahrani, and M. N. Al-Otaibi, *Cancer staging Manual*. 2016.

[8] E. K. Bartlett and G. C. Karakousis, "Current staging and prognostic factors in melanoma," *Surgical Oncology Clinics of North America*. 2015.

[9] P. V. Dickson and J. E. Gershenwald, "Staging and prognosis of cutaneous melanoma," *Surgical Oncology Clinics of North America*. 2011.

[10] W. Weyers, "Screening for malignant melanoma—a critical assessment in historical perspective," *Dermatol. Pract. Concept.*, 2018.

[11] R. J. Friedman, D. S. Rigel, and A. W. Kopf, "Early Detection of Malignant Melanoma: The Role of Physician Examination and Self-Examination of the Skin," *CA. Cancer J. Clin.*, 1985.

[12] N. R. Abbasi *et al.*, "Early diagnosis of cutaneous melanoma: Revisiting the ABCD criteria," *Journal of the American Medical Association*. 2004.

[13] S. N. Markovic *et al.*, "Malignant melanoma in the 21st century, part 1: Epidemiology, risk factors, screening, prevention, and diagnosis," in *Mayo Clinic Proceedings*, 2007.

[14] T. B. Fitzpatrick, "The Validity and Practicality of Sun-Reactive Skin Types I Through VI," *Arch. Dermatol.*, 1988.

[15] R. L. Barnhill and M. C. Mihm, "The histopathology of cutaneous malignant melanoma," *Seminars in Diagnostic*

Pathology. 1993.

[16] J. S. Goydos and S. L. Shoen, "Acral lentiginous melanoma," in *Cancer Treatment and Research*, 2016.

[17] J. A. Zell, P. Cinar, M. Mobasher, A. Ziogas, F. L. Meyskens, and H. Anton-Culver, "Survival for patients with invasive cutaneous melanoma among ethnic groups: The effects of socioeconomic status and treatment," *J. Clin. Oncol.*, 2008.

[18] P. Pisani, D. M. Parkin, F. Bray, and J. Ferlay, "Estimates of the worldwide mortality from 25 cancers in 1990," *Int. J. Cancer*, 1999.

[19] D. Schadendorf *et al.*, "Melanoma," *Nat. Rev. Dis. Prim.*, vol. 1, no. 1, p. 15003, 2015.

[20] B. Armstrong and A. Kricker, "How much melanoma is caused by sun exposure?," *Melanoma Res.*, 1993.

[21] F. Tas and K. Erturk, "Patient age and cutaneous malignant melanoma: Elderly patients are likely to have more aggressive histological features and poorer survival," *Mol. Clin. Oncol.*, 2017.

[22] C. M. Balch *et al.*, "Prognostic factors analysis of 17,600 melanoma patients: Validation of the American Joint Committee on Cancer melanoma staging system," *J. Clin. Oncol.*, 2001.

[23] C. M. Balch *et al.*, "Age as a prognostic factor in patients with localized melanoma and regional metastases," *Ann. Surg. Oncol.*, 2013.

[24] B. Pérez-Gómez, N. Aragonés, P. Gustavsson, V. Lope, G. López-Abente, and M. Pollán, "Do sex and site matter? Different age distribution in melanoma of the trunk among Swedish men and women," *Br. J. Dermatol.*, 2008.

[25] Z. Ali, N. Yousaf, and J. Larkin, "Melanoma epidemiology, biology and prognosis," in *European Journal of Cancer, Supplement*, 2013.

[26] J. L. Bulliard, B. Cox, and J. M. Elwood, "Latitude gradients in melanoma incidence and mortality in the non-Maori population of New Zealand," *Cancer Causes Control*, 1994.

[27] P. Valverde, E. Healy, I. Jackson, J. L. Rees, and A. J. Thody, "Variants of the melanocyte–stimulating hormone receptor gene are associated with red hair and fair skin in humans," *Nature Genetics*. 1995.

[28] A. J. Miller and M. C. Mihm, "Melanoma," *N. Engl. J. Med.*, vol. 355, no. 1, pp. 51–65, Jul. 2006.

[29] D. L., K. A.L., M. L., L. S.A., and A.-M. Z.A., "Melanocytes as instigators and victims of oxidative stress," *J. Invest. Dermatol.*, 2014.

[30] M. A. Pizzichetta *et al.*, "Amelanotic/hypomelanotic melanoma: Clinical and dermoscopic features," *Br. J. Dermatol.*, 2004.

[31] E. Erdei and S. M. Torres, "A new understanding in the epidemiology of melanoma," *Expert Review of Anticancer Therapy*. 2010.

[32] H. O. LANCASTER, "Some geographical aspects of the mortality from melanoma in Europeans," *Med. J. Aust.*, 1956.

[33] C. Garbe and U. Leiter, "Melanoma epidemiology and trends," *Clin. Dermatol.*, 2009.

[34] E. A. L. Enninga *et al.*, "Survival of cutaneous melanoma based on sex, age, and stage in the United States, 1992–2011," *Cancer Med.*, 2017.

[35] I. V. Fedorenko, K. H. T. Paraiso, and K. S. M. Smalley, "Acquired and intrinsic BRAF inhibitor resistance in BRAF V600E mutant melanoma," *Biochemical Pharmacology*. 2011.

[36] R. Schreck and U. R. Rapp, "Raf kinases: Oncogenesis and drug discovery," *International Journal of Cancer*. 2006.

[37] P. H. Warne, P. R. Vician, and J. Downward, "Direct interaction of Ras and the amino-terminal region of Raf-1 in vitro," *Nature*, 1993.

[38] A. B. Vojtek, S. M. Hollenberg, and J. A. Cooper, "Mammalian Ras interacts directly with the serine/threonine kinase raf," *Cell*, 1993.

[39] A. P. Kornev and S. S. Taylor, "Dynamics-Driven Allostery in Protein Kinases," *Trends in Biochemical Sciences*. 2015.

[40] J.-H. Pan *et al.*, "Development of small-molecule therapeutics and strategies for targeting RAF kinase in BRAF-mutant colorectal cancer," *Cancer Manag. Res.*, vol. 10, pp. 2289–2301, Aug. 2018.

[41] L. Palmieri and G. Rastelli, "αc helix displacement as a general approach for allosteric modulation of protein kinases," *Drug Discovery Today*. 2013.

[42] B. Y. Reddy, D. M. Miller, and H. Tsao, "Somatic driver mutations in melanoma," *Cancer*, vol. 123, no. S11, pp. 2104–2117, 2017.

[43] H. Davies *et al.*, "Mutations of the BRAF gene in human cancer," *Nature*, 2002.

[44] T. Ikenoue *et al.*, "Functional Analysis of Mutations within the Kinase Activation Segment of B-Raf in Human Colorectal Tumors," *Cancer Res.*, 2003.

[45] E. T. Kimura, M. N. Nikiforova, Z. Zhu, J. A. Knauf, Y. E. Nikiforov, and J. A. Fagin, "High prevalence of BRAF mutations in thyroid cancer: Genetic evidence for constitutive activation of the RET/PTC-RAS-BRAF signaling pathway in papillary thyroid carcinoma," *Cancer Res.*, 2003.

[46] R. Haq, D. E. Fisher, and H. R. Widlund, "Molecular

pathways: BRAF induces bioenergetic adaptation by attenuating oxidative phosphorylation," *Clin. Cancer Res.*, 2014.

[47] J. L. Manzano *et al.*, "Resistant mechanisms to BRAF inhibitors in melanoma," *Ann. Transl. Med.*, 2016.

[48] J. M. Junkins-Hopkins, "Malignant melanoma: Molecular cytogenetics and their implications in clinical medicine," *J. Am. Acad. Dermatol.*, 2010.

[49] G. Bollag *et al.*, "Vemurafenib: The first drug approved for BRAF-mutant cancer," *Nature Reviews Drug Discovery*. 2012.

[50] A. Hall *et al.*, "Dysfunctional oxidative phosphorylation makes malignant melanoma cells addicted to glycolysis driven by the V600EBRAF oncogene," *Oncotarget*, 2013.

[51] K. S. M. Smalley *et al.*, "CRAF inhibition induces apoptosis in melanoma cells with non-V600E BRAF mutations," *Oncogene*, 2009.

[52] J. A. Curtin *et al.*, "Distinct sets of genetic alterations in melanoma," *N. Engl. J. Med.*, 2005.

[53] B. Devitt *et al.*, "Clinical outcome and pathological features associated with NRAS mutation in cutaneous melanoma," *Pigment Cell Melanoma Res.*, 2011.

[54] E. Muñoz-Couselo, E. Z. Adelantado, C. Ortiz, J. S. García, and J. Perez-Garcia, "NRAS-mutant melanoma: Current challenges and future prospect," *OncoTargets and Therapy*. 2017.

[55] J. Thumar, D. Shahbazian, S. A. Aziz, L. B. Jilaveanu, and H. M. Kluger, "MEK targeting in N-RAS mutated metastatic melanoma," *Mol. Cancer*, 2014.

[56] M. Kiuru and K. J. Busam, "The NF1 gene in tumor syndromes and melanoma," *Laboratory Investigation*. 2017.

[57] R. Akbani *et al.*, "Genomic Classification of Cutaneous Melanoma," *Cell*, 2015.

[58] A. H. Shain *et al.*, "Exome sequencing of desmoplastic melanoma identifies recurrent NFKBIE promoter mutations and diverse activating mutations in the MAPK pathway," *Nat. Genet.*, 2015.

[59] M. Krauthammer *et al.*, "Exome sequencing identifies recurrent somatic RAC1 mutations in melanoma," *Nat. Genet.*, 2012.

[60] S. Rajkumar and I. R. Watson, "Molecular characterisation of cutaneous melanoma: Creating a framework for targeted and immune therapies," *British Journal of Cancer*. 2016.

[61] H. Cirenajwis *et al.*, "NF1-mutated melanoma tumors harbor distinct clinical and biological characteristics," *Mol. Oncol.*, 2017.

[62] B. Domingues, J. Lopes, P. Soares, and H. Populo,

"Melanoma treatment in review," *ImmunoTargets Ther.*, 2018.

[63] D. L. L. Roberts *et al.*, "U.K. guidelines for the management of cutaneous melanoma," *British Journal of Dermatology*. 2002.

[64] A. M. Eggermont, A. Spatz, and C. Robert, "Cutaneous melanoma," *Lancet*, vol. 383, no. 9919, pp. 816–827, Mar. 2014.

[65] P. Strojan, "Role of radiotherapy in melanoma management," *Radiology and Oncology*. 2010.

[66] M. R. Hamblin, Y. Y. Huang, D. Vecchio, P. Avci, R. Yin, and M. Garcia-Diaz, "Melanoma resistance to photodynamic therapy: New insights," *Biological Chemistry*. 2013.

[67] S. O. Gollnick, B. Owczarczak, and P. Maier, "Photodynamic therapy and anti-tumor immunity," *Lasers Surg. Med.*, 2006.

[68] I. Rafique, J. M. Kirkwood, and A. A. Tarhini, "Immune checkpoint blockade and interferon-α in melanoma," *Seminars in Oncology*. 2015.

[69] N. J. Ives *et al.*, "Adjuvant interferon-α for the treatment of high-risk melanoma: An individual patient data meta-analysis," *Eur. J. Cancer*, vol. 82, pp. 171–183, Sep. 2017.

[70] A. X. Torres-Collado, J. Knott, and A. R. Jazirehi, "Reversal of resistance in targeted therapy of metastatic melanoma: Lessons learned from vemurafenib (BRAFV600E-specific inhibitor)," *Cancers*. 2018.

[71] R. W. Joseph *et al.*, "Correlation of NRAS mutations with clinical response to high-dose IL-2 in patients with advanced melanoma," *Journal of Immunotherapy*. 2012.

[72] V. A. Trinh and B. Hagen, "Ipilimumab for advanced melanoma: A pharmacologic perspective," *J. Oncol. Pharm. Pract.*, 2013.

[73] G. Graziani, L. Tentori, and P. Navarra, "Ipilimumab: A novel immunostimulatory monoclonal antibody for the treatment of cancer," *Pharmacological Research*. 2012.

[74] Y. Heakal, M. Kester, and S. Savage, "Vemurafenib (PLX4032): An Orally Available Inhibitor of Mutated BRAF for the Treatment of Metastatic Melanoma," *Ann. Pharmacother.*, 2011.

[75] W. Zhang, D. Heinzmann, and J. F. Grippo, "Clinical Pharmacokinetics of Vemurafenib," *Clinical Pharmacokinetics*. 2017.

[76] J.-H. Pan *et al.*, "Development of small-molecule therapeutics and strategies for targeting RAF kinase in BRAF-mutant colorectal cancer," *Cancer Manag. Res.*, vol. 10, pp. 2289–2301, Aug. 2018.

[77] I. Arozarena and C. Wellbrock, "Overcoming resistance to

BRAF inhibitors," *Ann. Transl. Med. Vol 5, No 19 (October 2017) Ann. Transl. Med. (Focus "II Meet. Traslational Res. Melanoma by Spanish Melanoma Gr.*, 2017.

[78] U. M. Martens, "Small Molecules in Oncology," *Small Mol. Oncol.*, 2014.

[79] A. Swaika, J. A. Crozier, and R. W. Joseph, "Vemurafenib: An evidence-based review of its clinical utility in the treatment of metastatic melanoma," *Drug Design, Development and Therapy*. 2014.

[80] K. C. Hsu, "Improved outcome in HLA-identical sibling hematopoietic stem-cell transplantation for acute myelogenous leukemia predicted by KIR and HLA genotypes," *Blood*, vol. 105, pp. 4878–4884, 2005.

[81] S. M. Goldinger *et al.*, "A single-dose mass balance and metabolite-profiling study of vemurafenib in patients with metastatic melanoma," *Pharmacol. Res. Perspect.*, 2015.

[82] J. A. Sosman *et al.*, "Survival in BRAF V600-mutant advanced melanoma treated with vemurafenib," *N. Engl. J. Med.*, 2012.

[83] G. Bollag *et al.*, "Clinical efficacy of a RAF inhibitor needs broad target blockade in BRAF-mutant melanoma," *Nature*, 2010.

[84] P. B. Chapman *et al.*, "Improved survival with vemurafenib in melanoma with BRAF V600E mutation," *N. Engl. J. Med.*, 2011.

[85] and R. F. K. G.S. Falchook1, G.V. Long, R. Kurzrock, K.B. Kim, H.T. Arkenau, M.P. Brown, O. Hamid, J.R. Infante, M. Millward, A. Pavlick, S.J. O'Day, S.C. Blackman, C.M. Curtis, P. Lebowitz, B. Ma, D. Ouellet, "RAF Inhibitor Dabrafenib (GSK2118436) is Active in Melanoma Brain Metastases, Multiple BRAF Genotypes and Diverse Cancers," *Lancet*, 2012.

[86] K. T. Flaherty *et al.*, "Combined BRAF and MEK inhibition in melanoma with BRAF V600 mutations," *N. Engl. J. Med.*, 2012.

[87] J. Mangana, M. P. Levesque, M. B. Karpova, and R. Dummer, "Sorafenib in melanoma," *Expert Opin. Investig. Drugs*, 2012.

[88] S. M. Wilhelm, L. Adnane, P. Newell, A. Villanueva, J. M. Llovet, and M. Lynch, "Preclinical overview of sorafenib, a multikinase inhibitor that targets both Raf and VEGF and PDGF receptor tyrosine kinase signaling," *Molecular Cancer Therapeutics*. 2008.

[89] T. Lippert, H.-J. Ruoff, and M. Volm, "Intrinsic and Acquired Drug Resistance in Malignant Tumors," *Arzneimittelforschung*, 2011.

[90] R. Somasundaram, J. Villanueva, and M. Herlyn,

"Intratumoral Heterogeneity as a Therapy Resistance Mechanism. Role of Melanoma Subpopulations," in *Advances in Pharmacology*, 2012.

[91] K. Trunzer *et al.*, "Pharmacodynamic effects and mechanisms of resistance to vemurafenib in patients with metastatic melanoma," *J. Clin. Oncol.*, vol. 31, no. 14, pp. 1767–1774, 2013.

[92] F. Spagnolo, P. Ghiorzo, and P. Queirolo, "Overcoming resistance to BRAF inhibition in BRAF-mutated metastatic melanoma.," *Oncotarget*, vol. 5, no. 21, pp. 10206–21, 2014.

[93] M. Griffin *et al.*, "BRAF inhibitors: Resistance and the promise of combination treatments for melanoma," *Oncotarget*. 2017.

[94] H. Shi *et al.*, "Acquired resistance and clonal evolution in melanoma during BRAF inhibitor therapy," *Cancer Discov.*, vol. 4, no. 1, 2014.

[95] P. I. Poulikakos *et al.*, "RAF inhibitor resistance is mediated by dimerization of aberrantly spliced BRAF(V600E)," *Nature*, 2011.

[96] J. Villanueva *et al.*, "Acquired Resistance to BRAF Inhibitors Mediated by a RAF Kinase Switch in Melanoma Can Be Overcome by Cotargeting MEK and IGF-1R/PI3K," *Cancer Cell*, 2010.

[97] F. Spagnolo *et al.*, "BRAF-mutant melanoma: Treatment approaches, resistance mechanisms, and diagnostic strategies," *OncoTargets and Therapy*, vol. 8. pp. 157–168, 2015.

[98] E. Romano *et al.*, "Identification of multiple mechanisms of resistance to vemurafenib in a patient with BRAFV600E-mutated cutaneous melanoma successfully rechallenged after progression," *Clin. Cancer Res.*, 2013.

[99] R. Nazarian *et al.*, "Melanomas acquire resistance to B-RAF(V600E) inhibition by RTK or N-RAS upregulation," *Nature*, vol. 468, no. 7326, pp. 973–977, 2010.

[100] H. Shi *et al.*, "Melanoma whole-exome sequencing identifies V600E B-RAF amplification-mediated acquired B-RAF inhibitor resistance," *Nat. Commun.*, 2012.

[101] M. C. Mendoza, E. E. Er, and J. Blenis, "The Ras-ERK and PI3K-mTOR pathways: Cross-talk and compensation," *Trends in Biochemical Sciences*. 2011.

[102] F. Spagnolo, P. Ghiorzo, and P. Queirolo, "Overcoming resistance to BRAF inhibition in BRAF-mutated metastatic melanoma," *Oncotarget*, 2014.

[103] M. A. Davies, "The role of the PI3K-AKT pathway in melanoma," *Cancer Journal*. 2012.

[104] C. M. Johannessen *et al.*, "COT drives resistance to RAF inhibition through MAP kinase pathway reactivation,"

Nature, 2010.

[105] M. Cargnello and P. P. Roux, "Activation and Function of the MAPKs and Their Substrates, the MAPK-Activated Protein Kinases," *Microbiol. Mol. Biol. Rev.*, 2011.

[106] J. McCain, "The MAPK (ERK) Pathway: Investigational Combinations for the Treatment Of BRAF-Mutated Metastatic Melanoma," *P T*, vol. 38, no. 2, pp. 96–108, Feb. 2013.

[107] D. Hanahan and R. A. Weinberg, "The hallmarks of cancer," *Cell*. 2000.

[108] A. S. Dhillon, S. Hagan, O. Rath, and W. Kolch, "MAP kinase signalling pathways in cancer," *Oncogene*. 2007.

[109] T. J. Hemesath *et al.*, "microphthalmia, A critical factor in melanocyte development, defines a discrete transcription factor family," *Genes Dev.*, 1994.

[110] M. L. Hartman and M. Czyz, "MITF in melanoma: Mechanisms behind its expression and activity," *Cellular and Molecular Life Sciences*. 2015.

[111] C. Levy, M. Khaled, and D. E. Fisher, "MITF: master regulator of melanocyte development and melanoma oncogene," *Trends in Molecular Medicine*. 2006.

[112] S. Shibahara, "Microphthalmia-associated transcription factor (MITF): Multiplicity in structure, function, and regulation," *J. Investig. Dermatology Symp. Proc.*, 2001.

[113] E. M. Van Allen *et al.*, "The genetic landscape of clinical resistance to RAF inhibition in metastatic melanoma," *Cancer Discov.*, 2014.

[114] J. Müller *et al.*, "Low MITF/AXL ratio predicts early resistance to multiple targeted drugs in melanoma," *Nat. Commun.*, 2014.

[115] G. M. Fischer, Y. N. Vashisht Gopal, J. L. McQuade, W. Peng, R. J. DeBerardinis, and M. A. Davies, "Metabolic strategies of melanoma cells: Mechanisms, interactions with the tumor microenvironment, and therapeutic implications," *Pigment Cell and Melanoma Research*. 2018.

[116] M. G. Vander Heiden, L. C. Cantley, and C. B. Thompson, "Understanding the warburg effect: The metabolic requirements of cell proliferation," *Science*. 2009.

[117] D. A. Scott *et al.*, "Comparative metabolic flux profiling of melanoma cell lines: Beyond the Warburg effect," *J. Biol. Chem.*, 2011.

[118] P. Marchetti, A. Trinh, R. Khamari, and J. Kluza, "Melanoma metabolism contributes to the cellular responses to MAPK/ERK pathway inhibitors," *Biochimica et Biophysica Acta - General Subjects*. 2018.

[119] M. Barbi de Moura *et al.*, "Mitochondrial respiration - an important therapeutic target in melanoma," *PLoS One*,

2012.

[120] C. Pinheiro *et al.*, "The metabolic microenvironment of melanomas: Prognostic value of MCT1 and MCT4," *Cell Cycle*, 2016.

[121] E. Shtivelman *et al.*, "Pathways and therapeutic targets in melanoma," *Oncotarget*, 2014.

[122] T. Delgado-Goni *et al.*, "The BRAF inhibitor vemurafenib activates mitochondrial metabolism and inhibits hyperpolarized pyruvate-lactate exchange in BRAF-mutant human melanoma cells," *Mol. Cancer Ther.*, 2016.

[123] A. R. Baudy *et al.*, "FDG-PET is a good biomarker of both early response and acquired resistance in BRAFV600 mutant melanomas treated with vemurafenib and the MEK inhibitor GDC-0973," *EJNMMI Res.*, 2012.

[124] T. J. Parmenter *et al.*, "Response of BRAF-mutant melanoma to BRAF inhibition is mediated by a network of transcriptional regulators of glycolysis," *Cancer Discov.*, 2014.

[125] M. Leary, S. Heerboth, K. Lapinska, and S. Sarkar, "Sensitization of drug resistant cancer cells: A matter of combination therapy," *Cancers*. 2018.

[126] M. Holderfield, M. M. Deuker, F. McCormick, and M. McMahon, "Targeting RAF kinases for cancer therapy: BRAF-mutated melanoma and beyond," *Nature Reviews Cancer*. 2014.

[127] H. Helgadottir, I. R. Trocoli Drakensjö, and A. Girnita, "Personalized medicine in malignant melanoma: Towards patient tailored treatment," *Frontiers in Oncology*. 2018.

[128] R. Colla *et al.*, "Glutathione-mediated antioxidant response and aerobic metabolism: Two crucial factors involved in determining the multi-drug resistance of high-risk neuroblastoma," *Oncotarget*, 2016.

[129] P. M. Haverty *et al.*, "Reproducible pharmacogenomic profiling of cancer cell line panels," *Nature*, 2016.

[130] B. C. Heng *et al.*, "Effect of cell-seeding density on the proliferation and gene expression profile of human umbilical vein endothelial cells within ex vivo culture," *Cytotherapy*, 2011.

[131] M. McDermott *et al.*, "In vitro development of chemotherapy and targeted therapy drug-resistant cancer cell lines: A practical guide with case studies," *Front. Oncol.*, 2014.

[132] G. Wang, R. König, G. A. S. Ansari, and M. F. Khan, "Lipid peroxidation-derived aldehyde-protein adducts contribute to trichloroethene-mediated autoimmunity via activation of CD4+ T cells," *Free Radic. Biol. Med.*, 2008.

[133] E. Cappelli *et al.*, "Defects in mitochondrial energetic function compels Fanconi Anaemia cells to glycolytic

metabolism," *Biochim. Biophys. Acta - Mol. Basis Dis.*, 2017.

[134] G. Bianchi *et al.*, "Curcumin induces a fatal energetic impairment in tumor cells in vitro and in vivo by inhibiting ATP-synthase activity," *Carcinogenesis*, 2018.

[135] B. J. Altman, Z. E. Stine, and C. V Dang, "From Krebs to clinic: glutamine metabolism to cancer therapy.," *Nat. Rev. Cancer*, 2016.

[136] P. C. Hinkle, "P/O ratios of mitochondrial oxidative phosphorylation," *Biochimica et Biophysica Acta - Bioenergetics*. 2005.

[137] N. Thongon *et al.*, "Cancer cell metabolic plasticity allows resistance to NAMPT inhibition but invariably induces dependence on LDHA," *Cancer Metab.*, 2018.

[138] S. R. Chowdhury, J. Djordjevic, B. C. Albensi, and P. Fernyhough, "Simultaneous evaluation of substrate-dependent oxygen consumption rates and mitochondrial membrane potential by TMRM and safranin in cortical mitochondria," *Biosci. Rep.*, 2016.

[139] J. J. Hsiao and D. E. Fisher, "The roles of microphthalmia-associated transcription factor and pigmentation in melanoma," *Archives of Biochemistry and Biophysics*, vol. 563. pp. 28–34, 2014.

[140] C. R. Goding and H. Arnheiter, "MITF—the first 25 years," *Genes Dev.* , vol. 33, no. 15–16, pp. 983–1007, Aug. 2019.

[141] P. C. Hinkle, "P/O ratios of mitochondrial oxidative phosphorylation," *Biochim. Biophys. Acta - Bioenerg.*, vol. 1706, no. 1, pp. 1–11, 2005.

[142] D. M. Parkin, P. Pisani, and J. Ferlay, "Global cancer statistics," *CA. Cancer J. Clin.*, 1999.

[143] F. Spagnolo, P. Ghiorzo, and P. Queirolo, "Overcoming resistance to BRAF inhibition in BRAF-mutated metastatic melanoma.," *Oncotarget*, vol. 5, no. 21, pp. 10206–21, 2014.

[144] J. Larkin *et al.*, "Combined vemurafenib and cobimetinib in BRAF-mutated melanoma," *N. Engl. J. Med.*, 2014.

[145] J. N. Søndergaard *et al.*, "Differential sensitivity of melanoma cell lines with BRAFV600Emutation to the specific Raf inhibitor PLX4032," *J. Transl. Med.*, 2010.

[146] J. E. Hernandez-Davies *et al.*, "Vemurafenib resistance reprograms melanoma cells towards glutamine dependence," *J. Transl. Med.*, 2015.

[147] V. Fritz and L. Fajas, "Metabolism and proliferation share common regulatory pathways in cancer cells," *Oncogene*. 2010.

[148] S. Bonnet *et al.*, "A Mitochondria-K+ Channel Axis Is Suppressed in Cancer and Its Normalization Promotes Apoptosis and Inhibits Cancer Growth," *Cancer Cell*, 2007.

[149] D. Hanahan and R. A. Weinberg, "Hallmarks of cancer: The

_____

next generation," *Cell*. 2011.

[150] K. Yizhak *et al.*, "A computational study of the Warburg effect identifies metabolic targets inhibiting cancer migration," *Mol. Syst. Biol.*, 2014.

[151] R. Haq *et al.*, "Oncogenic BRAF regulates oxidative metabolism via PGC1α and MITF," *Cancer Cell*, vol. 23, no. 3, pp. 302–315, 2013.

[152] P. Corazao-rozas *et al.*, "Mitochondrial oxidative stress is the achille ' s heel of melanoma cells resistant to Braf-mutant inhibitor ABSTRACT :," vol. 4, no. 11, 2013.

[153] E. Piskounova *et al.*, "Oxidative stress inhibits distant metastasis by human melanoma cells," *Nature*, 2015.

[154] N. Traverso *et al.*, "Role of glutathione in cancer progression and chemoresistance.," *Oxid. Med. Cell. Longev.*, vol. 2013, p. 972913, Jan. 2013.